Gibbs phenomenon

Theoretical understanding and Resolution of the Gibbs phenomenon

by

Milou Dijk

to obtain the degree of Bachelor of Science

at the Delft University of Technology,

to be defended publicly on Wednesday June 26, 2024 at 10:00 AM.

Student number:	5408873	
Project duration:	April, 2024 – June, 2024	
Thesis committee:	Dr. F. Bartolucci,	TU Delft, supervisor
	Prof. dr. D. C. Gijswijt	TU Delft

TU Delft

Lay summary

In this thesis, the Gibbs phenomenon will be investigated. Specifically, what is the Gibbs phenomenon, when it occurs and why it is important to investigate this phenomenon.
Signals can be described by a sum of simple sine and cosine waves, known as Fourier series. When we approximate a signal that contains a “jump” with finitely many terms in the Fourier series, something interesting happens: around the “jump” we can see a ripple - a peak followed by rapid oscillations - that was not present in the original signal.
In general, if we consider more terms in the Fourier series we would expect this ripple to vanish. However, the observation that this peak will never decrease below 9% of the height of the “jump” is exactly what we call the Gibbs phenomenon.
Several methods will be discussed in order to remove this phenomenon and finally we will look into its occurrence (and its resolution) in Magnetic Resonance Imaging.

Milou Dijk
Delft, June 2024

Abstract

In short, the Gibbs phenomenon describes the oscillating behaviour followed by an overshoot or undershoot of a Fourier partial sum expansion compared to the original function near jump discontinuities. In particular, the fact that this overshoot or undershoot will never decrease below 9% of the height of the "jump".

First, some historical remarks about the discovery of the Gibbs phenomenon are given and several fundamental elements of Fourier analysis are introduced. By thoroughly analyzing the Saw-tooth wave function, an example of a function that exhibits the Gibbs phenomenon, we provide some figures in order to visualize this phenomenon. Furthermore, we address and fill in the gaps of the existing mathematical proof to advance the theoretical understanding of the Gibbs phenomenon. This analysis is then generalized to apply to a broader class of functions with jump discontinuities, by first considering a function with a jump discontinuity at 0 and then proving the occurrence of the phenomenon at a general point of jump discontinuity.

Furthermore, a literature research is conducted to evaluate different methods for resolving the Gibbs phenomenon. This thesis includes an in-depth analysis of filtering methods and spectral reprojection methods. Specifically, the Gegenbauer reconstruction method is described and its theoretical foundations in removing the Gibbs phenomenon is examined. Finally, a real-life application of the Gibbs phenomenon is given by looking at its occurrence in Magnetic Resonance Imaging.

Overall, this thesis not only advances the theoretical understanding of the Gibbs phenomenon but also provides an insight into its resolution and application in Magnetic Resonance Imaging.

Milou Dijk
Delft, June 2024

Contents

Nomenclature

Abbreviations

Abbreviation	Definition
MRI	Magnetic Resonance Imaging

Symbols

Symbol	Definition
$\mathbb{N}$	Natural numbers
$\mathbb{R}$	Real numbers
$\mathbb{C}$	Complex numbers
$\mathbb{T}$	Torus
N	Number of Fourier coefficients
$S_N[f](x)$	Nth Partial Fourier sum of function $f(x)$
$\hat{f}_n$	nth Fourier coefficient
$\mathcal{O}$	Order of convergence
C^p	Continuous function with p derivatives
L^1	Banach space w.r.t. the norm $\|\|x\|\|_1 = \sum \|x_i\|$
L^2	Hilbert space w.r.t. the norm $\|\|x\|\|_2 = \sqrt{\sum \|x_i\|^2}$

1 Introduction

Any signal can be rewritten as the sum of a series of simple sine and cosine waves. By adding together all these simpler waves with varying combinations of frequencies and amplitudes, the Fourier series, we can recover the original signal.

If we consider a function f that has a jump discontinuity at a certain point t_0 and we draw a graph of the partial sum of the Fourier series of this function, a typical behaviour can be observed, see for instance Figure 1.1. As t approaches the point of discontinuity t_0, the graph of the partial Fourier sum $S_N[f](t)$ somehow oscillates right before the jump and when the jump is accomplished, it overshoots and then calms down again.

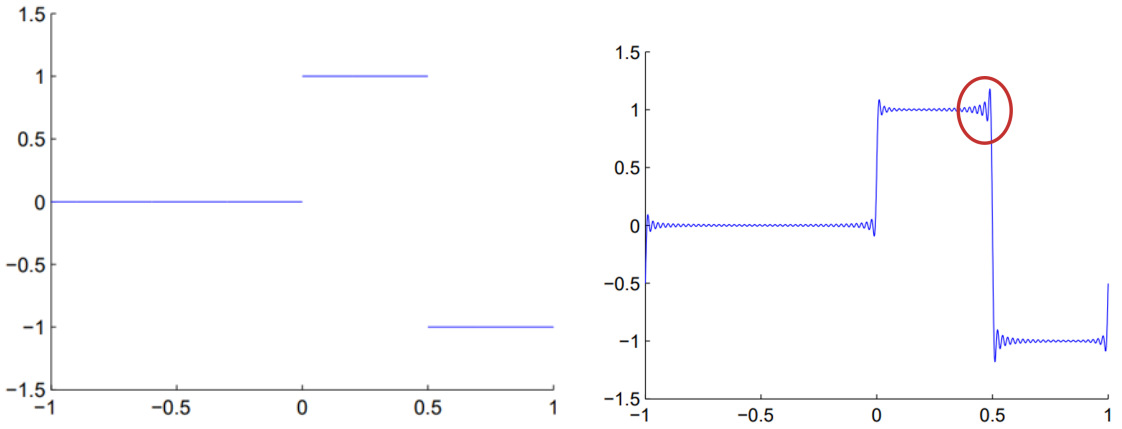

(a) Square wave function

(b) Fourier series approximation of Square wave function

Figure 1.1: Gibbs phenomenon. Image from [2].

During the nineteenth century this sort of behaviour was observed by experimental physicists. At that time it was considered as an error of the measuring equipment. However, number of mathematicians showed this is not the case and that we are dealing with an actual mathematical phenomenon. This behaviour is named after J.W. Gibbs, and has an extensive history.

Historical remarks

The first known study on the observation of the oscillatory behaviour of partial sums of Fourier series near discontinuities was carried out by H. Wilbraham in 1848 [13]. Remarkably, this paper was never properly appreciated and seemed forgotten.
In 1898, A. A. Michelson wrote a letter to *Nature* in which he criticized the idea that a series of continuous functions could converge to a discontinuous function. He investigated the function

$$g(x) = \frac{1}{2}x$$

corresponding to the series

$$g(x) = \sum_{k=1}^{\infty} \frac{(-1)^{k+1}}{k} \sin(kx)$$

in order to substantiate his criticism. However, he lacked understanding of the difference between the sum of an infinite series and the partial sums of such a series.
Hence, in the next issue of *Nature*, the mathematician A. Love pointed out Michelson's lack of understanding. This is when J.W. Gibbs joined the discussion by writing a letter in which he tried to clarify Love's remark, by stating that the graph of the limit is not necessarily the same as the limit of the graphs (of the partial sums of Fourier series) [5]. In other words, the Fourier series converges point-wise to the function, but this does not imply that the graphs of the partial sums need to look like the graph of the function as $N \to \infty$. Furthermore, Gibbs published a second letter in which he mentioned the quantity

$$\mathrm{Si}(x) = \int_0^x \frac{\sin(t)}{t} dt.$$

This sine integral function plays an important role in determining the amount of overshoot in the convergence of the partial sums of Fourier series near discontinuities. However, Gibbs did not provide any proofs or calculations of this overshoot near discontinuities.
Only after seven years since Gibbs first publication, the term "Gibbs phenomenon" was introduced by M. Bôcher [3]. Bôcher performed a detailed analysis on the function

$$f(x) = \frac{1}{2}(\pi - x)$$

for $0 < x < 2\pi$ which can be described by

$$f(x) = \sum_{k=1}^{\infty} \frac{\sin(kx)}{k}.$$

He also provided the complete proof of Gibbs' assertion.
Towards the end of 1914, H. Burkhardt mentioned the long-forgotten work of H. Wilbraham, who already discovered the Gibbs phenomenon in 1848. Hence, he argued it would be more appropriate to call the observation discussed here the "Wilbraham-Gibbs phenomenon".

Structural overview

In Chapter 2 some fundamental theorems and definitions of Fourier analysis will be introduced. Moreover, some important convergence results will be stated. Chapter 3 will consist of a detailed analysis of the Saw-tooth wave function and the mathematical proof of the Gibbs phenomenon.
This result will be generalized in Chapter 4, by considering a function with a jump discontinuity at 0 and then proving the occurrence of the phenomenon at a general point of jump discontinuity.

The second part of this thesis focuses on the resolution of the Gibbs phenomenon. In Chapter 5, several techniques - such as filtering and spectral reprojection methods - to improve the convergence rate will be reviewed.
The Gegenbauer reconstruction method, an example of a spectral reprojection method, will be investigated in Chapter 6. In Chapter 7 we will look at the occurrence of Gibbs ringing artifact in Magnetic Resonance Imaging and describe the hybrid Gegenbauer method in order to resolve this artifact. To finalize, Chapter 8 will consist of the main conclusions and some suggestions for further research.

2

Preliminary theory

In this chapter some definitions and theorems of Fourier analysis are reviewed that will be used in this report. These definitions and theorems with their proofs can be found in references [9], [10] and [12].

Fourier series

The Gibbs phenomenon occurs when we consider the partial Fourier sums of a certain class of functions. These functions are piecewise continuous except for a finite number of points in which the function "jumps" from a certain value to another.

Definition 2.1. Let $a, b \in \mathbb{R}$. A function $f : [a, b] \to \mathbb{C}$ is called piecewise continuous if there exist $a = a_0 \leq a_1 \leq ... \leq a_n = b$ such that f is continuous on (a_j, a_{j+1}) for $j = 0, 1, ..., n-1$ and the limits $f'(a_j^+)$ and $f'(a_j^-)$ exist and are finite for all $j = 0, 1, ..., n-1$.

Definition 2.2. A function $f(x)$ has a jump discontinuity at $x = a$, if we have $f(a^+) = \lim_{x \to a^+} f(x) < \infty$, $f(a^-) = \lim_{x \to a^-} f(x) < \infty$, and $f(a^+) \neq f(a^-)$.

Definition 2.3. Suppose $f : \mathbb{T} \to \mathbb{C}$ integrable and 2π periodic. Then the nth Fourier coefficient of f is defined by

$$\hat{f}(n) = \frac{1}{2\pi} \int_{-\pi}^{\pi} f(\theta) e^{-in\theta} d\theta.$$

Definition 2.4. Let $f : \mathbb{T} \to \mathbb{C}$ integrable and 2π periodic and $\hat{f}(n)$ be the Fourier coefficients of f as in Definition 2.3. Then the Fourier series of f is defined by

$$\sum_{n=-\infty}^{\infty} \hat{f}(n) e^{in\theta} = \frac{a_0}{2} + \sum_{n=1}^{\infty} \left[a_n \cos(n\theta) + b_n \sin(n\theta) \right], \tag{2.1}$$

where a_n and b_n are given by

$$a_n = \frac{1}{\pi} \int_{-\pi}^{\pi} f(\theta) \cos(n\theta) d\theta \tag{2.2}$$

and

$$b_n = \frac{1}{\pi} \int_{-\pi}^{\pi} f(\theta) \sin(n\theta) d\theta. \tag{2.3}$$

Definition 2.5. Let $f : \mathbb{T} \to \mathbb{C}$ integrable and 2π periodic. Then we define the Nth partial Fourier sum of f as

$$S_N[f](\theta) = \sum_{n=-N}^{N} \hat{f}(n) e^{in\theta}.$$

Dirichlet kernel

The Dirichlet kernel has some important properties useful for analysis of the partial Fourier sums of certain functions.

Definition 2.6. The Dirichlet kernel is a trigonometric polynomial of degree N defined by

$$D_N(t) = \sum_{n=-N}^{N} e^{int}.$$

If we use the fact that $e^{int} + e^{-int} = 2\cos(nt)$, the Dirichlet kernel can also be written as

$$D_N(t) = 1 + 2\sum_{n=1}^{N} \cos(nt). \tag{2.4}$$

Another expression of the Dirichlet kernel in terms of the sine function is given by

$$D_N(t) = \frac{\sin\left((2N+1)\frac{t}{2}\right)}{\sin\left(\frac{t}{2}\right)} \quad \text{for} \quad t \notin 2\pi\mathbb{Z}. \tag{2.5}$$

Proof. Suppose $t \notin 2\pi\mathbb{Z}$. Then $e^{it} \neq 1$ and we get

$$D_N(t) = \sum_{n=-N}^{N} e^{int} = e^{-iNt}(1 + e^{it} + ... + e^{2iNt}).$$

This is a finite geometric series, so we get

$$\begin{aligned} D_N(t) &= e^{-iNt}\left(\frac{1 - e^{i(2N+1)t}}{1 - e^{it}}\right) \\ &= \frac{e^{-iNt} - e^{i(N+1)t}}{1 - e^{it}} \\ &= \frac{e^{-i\left(N+\frac{1}{2}\right)t} - e^{i\left(N+\frac{1}{2}\right)t}}{e^{-\frac{1}{2}it} - e^{\frac{1}{2}it}} \\ &= \frac{\sin\left(\left(N+\frac{1}{2}\right)t\right)}{\sin\left(\frac{t}{2}\right)} \\ &= \frac{\sin\left((2N+1)\frac{t}{2}\right)}{\sin\left(\frac{t}{2}\right)}. \end{aligned}$$

□

Definition 2.7. Let $f, g : \mathbb{T} \to \mathbb{C}$ be 2π periodic and integrable functions. Then their convolution $f * g$ on $\mathbb{T}$ is defined as

$$(f * g)(\theta) = \frac{1}{2\pi}\int_{-\pi}^{\pi} g(\theta - y)f(y)dy.$$

Important properties of the Dirichlet kernel are stated in Theorem 2.1.

Theorem 2.1. *Let $f : \mathbb{T} \to \mathbb{C}$ be integrable and $t \in \mathbb{R}$. Then the following holds:*

(i) $S_N[f](t) = (D_N * f)(t)$

(ii) D_N *is an even function*

(iii) $\frac{1}{2\pi}\int_{\pi}^{\pi} D_N(t)dt = 1$

Proof. (i) From the definition of the convolution we get

$$(D_N * f)(t) = \frac{1}{2\pi} \int_{-\pi}^{\pi} D_N(t-\tau) f(\tau) d\tau.$$

Now using the definition of the Dirichlet kernel we obtain

$$\begin{aligned}
(D_N * f)(t) &= \frac{1}{2\pi} \int_{-\pi}^{\pi} \left[\sum_{n=-N}^{N} e^{in(t-\tau)} \right] f(\tau) d\tau \\
&\overset{*}{=} \sum_{n=-N}^{N} e^{int} \left(\frac{1}{2\pi} \int_{-\pi}^{\pi} e^{-in\tau} f(\tau) d\tau \right) \\
&= \sum_{n=-N}^{N} e^{int} \hat{f}(n) \\
&= S_N[f](t).
\end{aligned}$$

Since we have a bounded summand the Dominated Convergence Theorem can be used to switch the integral and sum in step (*).
(ii) Trivial, since from expression (2.4) it is clear that we have $D_N(t) = D_N(-t)$.
(iii) Consider the integral

$$\begin{aligned}
\frac{1}{2\pi} \int_{-\pi}^{\pi} D_N(t) dt &\overset{(ii)}{=} \frac{1}{\pi} \int_{0}^{\pi} D_N(t) dt \\
&\overset{(2.4)}{=} \frac{1}{\pi} \int_{0}^{\pi} \left[1 + 2 \sum_{n=1}^{N} \cos(nt) \right] dt \\
&= \frac{1}{\pi} \cdot \pi + 2 \int_{0}^{\pi} \left[\cos(t) + \cos(2t) + ... + \cos(Nt) \right] dt \\
&= 1.
\end{aligned}$$

□

Convergence results

In order to investigate the behaviour of the partial sums near discontinuities it is important to consider some general convergence results regarding the Fourier series.

The Riemann-Lebesgue Lemma, stated in Lemma (A.1) shows that for functions $f \in L^1(\mathbb{T})$ the Fourier coefficients of f decay to zero as $|n|$ tends to ∞.

Lemma 2.1. *Let $-\infty \leq a < b \leq \infty$ and $f \in L^1(a,b)$. Then*

$$\lim_{|\lambda| \to \infty} \int_a^b f(x) e^{-i\lambda t} dt = 0.$$

In particular, if $f \in L^1(\mathbb{T})$, then $\hat{f}(n) \to 0$ as $|n| \to \infty$.

The formal proof of the Riemann-Lebesgue Lemma can be found in Appendix A.1.

Furthermore, it is important to mention the definition of α-Hölder continuity since 'normal' continuity is not a sufficient condition for (uniform) convergence of the partial Fourier sum.

Definition 2.8. Let $f(x)$ be a 2π periodic function in $L^1(-\pi, \pi)$. Then f is α-Hölder continuous at x_0 with order $\alpha > 0$, if there exists a constant $M > 0$ such that $|f(x) - f(x_0)| \leq M|x - x_0|^\alpha$ in a neighborhood of x_0. If the condition holds for all x_0 with the same constant M, then f is uniformly α-Hölder continuous.

Note that α-Hölder continuity with $\alpha = 1$ can be considered as Lipschitz continuity.

Theorem 2.2. *Let $f \in L^1(-\pi, \pi)$. Suppose that there exists $x \in \mathbb{R}$ such that the left- and right- limits $f(x^+)$ and $f(x^-)$ exist. Moreover assume that there exist $M > 0$, $\alpha > 0$ and $\delta > 0$ such that*

$$|f(x+t) - f(x^+)| \leq Mt^\alpha, \quad |f(x-t) - f(x^-)| \leq Mt^\alpha$$

for $0 < t < \delta$. Then

$$S_N[f](x) \to \frac{1}{2}(f(x^+) + f(x^-)) \quad \text{as} \quad N \to \infty.$$

3

Gibbs phenomenon

Piecewise continuous functions are functions that are continuous at every point in their domain except at finitely many points at which they have jump discontinuities, i.e. the left- and right-hand limits of the function exist but are not equal. Due to their abrupt changes between two values, piecewise continuous functions pose challenges in signal processing.
It is well known that periodic piecewise continuous functions can be represented as infinite sums of sine and cosine waves, known as Fourier series. As we delve deeper into the convergence of the partial sums of the Fourier series, we encounter a particular behaviour near jump discontinuities, the so-called Gibbs phenomenon. We will investigate this phenomenon for the Saw-tooth wave function, see Figure 3.1. Despite its simplicity, the Saw-tooth function serves as an example to observe this behaviour and to give a formal mathematical proof of the Gibbs phenomenon.

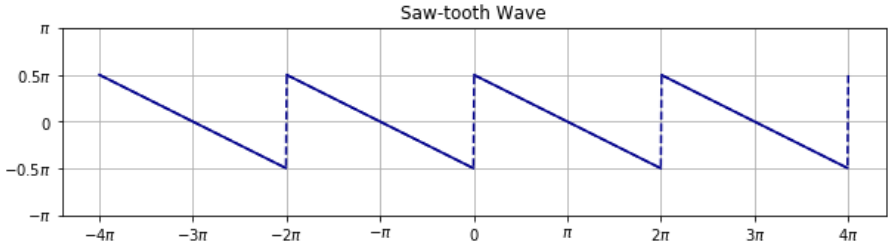

Figure 3.1: This figure displays the Saw-tooth wave function $f(x) = \frac{1}{2}(\pi - x)$ for $0 < x < 2\pi$.

This phenomenon is often referred to as the “overshoot” in the partial sums of Fourier series around “jumps”. However, the behaviour of the partial sums near jump discontinuities appears to be more complicated than just an overshoot.

3.1. Fourier series expansion of Saw-tooth wave function

We consider the Saw-tooth wave function, which is the 2π-periodic function defined by $f(x) = \frac{1}{2}(\pi - x)$ for $0 < x < 2\pi$. Then, we use formula (2.1) to compute its Fourier series. Since the Saw-tooth wave function is odd, we expect a pure sine expansion. Indeed, by using integrating by parts, we find

$$\begin{aligned} a_n &= \frac{1}{\pi}\int_0^{2\pi} \frac{1}{2}(\pi - x)\cos(nx)dx \\ &= \frac{1}{2}\int_0^{2\pi} \cos(nx)dx - \frac{1}{2\pi}\int_0^{2\pi} x\cos(nx)dx \\ &= 0 - \frac{1}{2\pi}\left(x\frac{\sin(nx)}{n}\Big|_0^{2\pi} - \int_0^{2\pi} \frac{\sin(nx)}{n}dx \right) \\ &= 0, \end{aligned} \tag{3.1}$$

while

$$\begin{aligned} b_n &= \frac{1}{\pi}\int_0^{2\pi} \frac{1}{2}(\pi - x)\sin(nx)dx \\ &= \frac{1}{2}\int_0^{2\pi} \sin(nx)dx - \frac{1}{2\pi}\int_0^{2\pi} x\sin(nx)dx \\ &= 0 - \frac{1}{2\pi}\left(-x\frac{\cos(nx)}{n}\Big|_0^{2\pi} + \int_0^{2\pi} \frac{\cos(nx)}{n}dx \right) \\ &= -\frac{1}{2\pi}\cdot -\frac{2\pi}{n} \\ &= \frac{1}{n}. \end{aligned} \tag{3.2}$$

Thus, we get the following Fourier series expansion

$$\sum_{n=1}^{\infty} \frac{\sin(nx)}{n}. \tag{3.3}$$

So that, the Nth partial Fourier sum of f is

$$S_N[f](x) = \sum_{n=1}^{N} \frac{\sin(nx)}{n}. \tag{3.4}$$

We observed that S_N is 2π-periodic, $S_N(-x) = -S_N(x)$ and $S_N(0) = S_N(\pi) = 0$. Thus, it is sufficient to completely study the behavior of S_N by looking at the interval $(0, \pi)$.

3.2. Convergence of partial Fourier sums

In order to describe the convergence of $S_N(x)$ to its sum $\frac{1}{2}(\pi - x)$ in the interval $(0, \pi)$, it suffices to show that the integral I_N defined in (3.5) is bounded.

Integral I_N

Define the integral I_N by

$$I_N = \int_0^\pi \sin\left(\left(N + \frac{1}{2}\right)t\right)\left[\frac{1}{2\sin\left(\frac{1}{2}t\right)} - \frac{1}{t}\right] dt. \tag{3.5}$$

Denote the part in square brackets by $g(t)$. In order to apply the second mean value theorem for integrals, it is enough to show that $g(t)$ is continuous in the interval $(0, \pi)$.

According to the second mean value theorem for integrals there is a number $0 < \xi < \pi$ for which we have

$$\begin{aligned} I_N &= g(0)\int_0^\xi \sin\left(\left(N + \frac{1}{2}\right)t\right) dt + g(\pi)\int_\xi^\pi \sin\left(\left(N + \frac{1}{2}\right)t\right) dt \\ &= \left(\frac{1}{2} - \frac{1}{\pi}\right)\int_\xi^\pi \sin\left(\left(N + \frac{1}{2}\right)t\right) dt \\ &= \left(\frac{1}{2} - \frac{1}{\pi}\right)\frac{1}{N + \frac{1}{2}}\cos\left(\left(N + \frac{1}{2}\right)\xi\right). \end{aligned}$$

Thus, if we consider the bound $|I_N|$, we can use the fact that $|\cos(x)| \leq 1$ for all x, to obtain a bound for the integral I_N.

Sine integral function

As mentioned in the introduction, Gibbs analysed the quantity

$$\mathrm{Si}(x) = \int_0^x \frac{\sin(t)}{t} dt. \tag{3.6}$$

The sine integral function is known to converge to $\frac{1}{2}\pi$, as shown graphically in Figure 3.2.

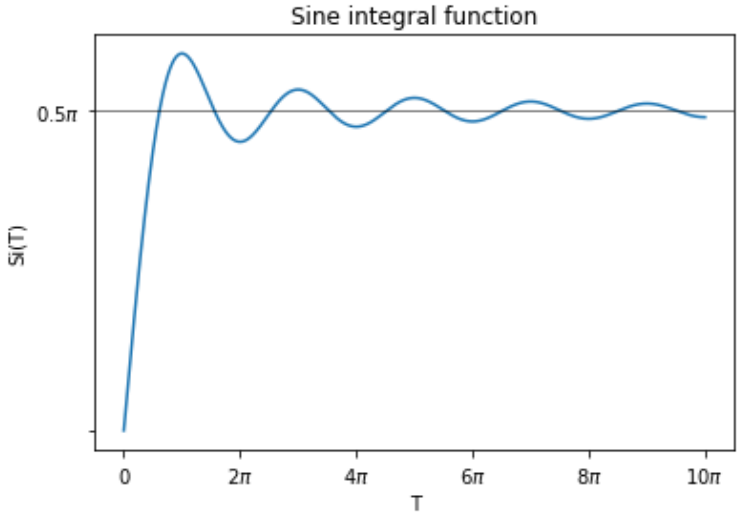

Figure 3.2: This figure displays the convergence of Si(T) as $T \to \infty$.

The mathematical proof establishing the convergence of the sine integral function is described in Theorem 3.1.

Theorem 3.1. *The function Si(x) converges to* $\frac{1}{2}\pi$ *as* $x \to \infty$*, i.e.* $\lim_{x\to\infty} Si(x) = \frac{1}{2}\pi$.

Proof. By direct computation, we have that

$$\begin{aligned}
0 &= S_N(\pi) - S_N(0) \\
&\overset{(1)}{=} \int_0^\pi S_N'(t)\,dt \\
&\overset{(2)}{=} \int_0^\pi \frac{\sin\left(\frac{1}{2}Nt\right)\cos\left(\frac{1}{2}(N+1)t\right)}{\sin\left(\frac{1}{2}t\right)}dt \\
&\overset{(3)}{=} \int_0^\pi \frac{\sin\left(-\frac{1}{2}t\right) + \sin\left((N+\frac{1}{2})t\right)}{2\sin\left(\frac{1}{2}t\right)}dt \\
&= \int_0^\pi \left(\frac{\sin\left((N+\frac{1}{2})t\right)}{2\sin\left(\frac{1}{2}t\right)} - \frac{1}{2}\right)dt.
\end{aligned}$$

The first step follows from the fundamental theorem of calculus.
In the second step, the expression of the first-derivative from (3.8) is used.
We apply the trigonometric identity $\sin(x)\cos(y) = \frac{1}{2}\left(\sin(x+y) + \sin(x-y)\right)$ in step (3) to obtain the desired expression for the integral.
Finally, by linearity of the integral, we get

$$\int_0^\pi \frac{\sin\left((N+\frac{1}{2})t\right)}{2\sin\left(\frac{1}{2}t\right)}dt = \int_0^\pi \frac{1}{2}dt,$$

which gives us the following result

$$\int_0^\pi \frac{\sin\left((N+\frac{1}{2})t\right)}{2\sin\left(\frac{1}{2}t\right)}dt = \frac{1}{2}\pi. \tag{3.7}$$

Hence, we showed that the integral Si(x) converges to $\frac{1}{2}\pi$. □

By using these results and preliminary theorems about convergence of partial sums of Fourier series, we obtain the following result.

Theorem 3.2. $\lim_{N\to\infty} S_N(x) = \frac{1}{2}(\pi - x)$ *for* $0 < x < \pi$.

Proof. By direct computation, we get

$$\begin{aligned}
S_N(x) &= \int_0^x S_N'(t)dt \\
&\overset{(1)}{=} \int_0^x \left(\frac{\sin\left((N+\frac{1}{2})t\right)}{2\sin\left(\frac{1}{2}t\right)} - \frac{1}{2}\right)dt \\
&\overset{(2)}{=} \int_0^x \frac{\sin\left((N+\frac{1}{2})t\right)}{2\sin\left(\frac{1}{2}t\right)}dt - \int_0^x \frac{1}{2}dt \\
&\overset{(3)}{=} \int_0^x \left(\frac{\sin\left((N+\frac{1}{2})t\right)}{2\sin\left(\frac{1}{2}t\right)} - \frac{\sin\left((N+\frac{1}{2})t\right)}{t} + \frac{\sin\left(\left(N+\frac{1}{2}\right)t\right)}{t}\right)dt - \frac{1}{2}x \\
&= \int_0^x \sin\left(\left(N+\frac{1}{2}\right)t\right)\left[\frac{1}{2\sin(\frac{1}{2}t)} - \frac{1}{t}\right]dt + \int_0^x \frac{\sin\left((N+\frac{1}{2})t\right)}{t}dt - \frac{1}{2}x \\
&= I_N(x) + \int_0^x \frac{\sin\left((N+\frac{1}{2})t\right)}{t}dt - \frac{1}{2}x \\
&= I_N(x) + \int_0^{(N+\frac{1}{2})x} \frac{\sin(t)}{t}dt - \frac{1}{2}x.
\end{aligned}$$

Step (1) follows from (3.7). Then, we use linearity of the integral in step (2). By adding and subtracting the term $\frac{\sin\left(\left(N+\frac{1}{2}\right)t\right)}{t}$ in the third line we can rewrite the integral in terms of I_N, defined in (3.5).

Now if we consider the limit of the partial sum we obtain

$$\begin{aligned}
\lim_{N\to\infty} S_N(x) &= \lim_{N\to\infty} I_N(x) + \int_0^{(N+\frac{1}{2})x} \frac{\sin(t)}{t} dt - \frac{1}{2}x \\
&\overset{\text{(Thm 3.4)}}{=} 0 + \lim_{T\to\infty} \int_0^T \frac{\sin(t)}{t} dt - \frac{1}{2}x \\
&\overset{(3.6)}{=} \lim_{T\to\infty} \mathrm{Si}(t) - \frac{1}{2}x \\
&\overset{\text{(Thm 3.1)}}{=} \frac{1}{2}\pi - \frac{1}{2}x = \frac{1}{2}(\pi - x),
\end{aligned}$$

which concludes the proof. □

3.3. Mathematical proof of Gibbs phenomenon

We start considering the Nth partial sum S_N of the Fourier series of the Saw-tooth wave function and determine its local maxima and minima. We observe that, as we consider more terms in the partial sum, i.e. as N tends to ∞, the first minimum and maximum tend to zero and the partial sums at these extreme points converge to certain values of the sine integral function. Several auxiliary results need to be proved in order to show such a behaviour of the partial sums. Finally, we use the sine integral function in order to compute the amount of overshoot and undershoot near the jump discontinuities.

3.3.1. Determining extreme points

First of all, we need to find the local maxima and minima of S_N by computing $S'_N(x) = 0$.

$$\begin{aligned}
S'_N(x) &= \sum_{k=1}^{N} \cos(kx) \\
&= \frac{1}{2\sin\left(\frac{1}{2}x\right)} \sum_{k=1}^{N} 2\sin\left(\frac{1}{2}x\right)\cos(kx) \\
&= \frac{1}{2\sin\left(\frac{1}{2}x\right)} \sum_{k=1}^{N} \left[\sin\left(\frac{1}{2}x + kx\right) + \sin\left(\frac{1}{2}x - kx\right)\right] \\
&= \frac{1}{2\sin\left(\frac{1}{2}x\right)} \sum_{k=1}^{N} \sin\left(\left(k+\frac{1}{2}\right)x\right) + \sin\left(\left(k-\frac{1}{2}\right)x\right) \\
&= \frac{1}{2\sin\left(\frac{1}{2}x\right)} \left[\sum_{k=1}^{N} \sin\left(\left(k+\frac{1}{2}\right)x\right) - \sum_{k=0}^{N-1} \sin\left(\left(k+\frac{1}{2}\right)x\right)\right] \\
&= \frac{1}{2\sin\left(\frac{1}{2}x\right)} \left[\sin\left(\left(N+\frac{1}{2}\right)x\right) - \sin\left(\frac{1}{2}x\right)\right].
\end{aligned}$$

By using the trigonometric identity $\sin(x) - \sin(y) = 2\left[\sin\left(\frac{x-y}{2}\right)\cos\left(\frac{x+y}{2}\right)\right]$, we obtain the following equation

$$S'_N(x) = \frac{\sin\left(\frac{1}{2}Nx\right)\cos\left(\frac{1}{2}(N+1)x\right)}{\sin\left(\frac{1}{2}x\right)}. \tag{3.8}$$

The zeros of $S'_N(x)$ in $(0,\pi)$ can be obtained from equation (3.8). If we consider the interval $\left(\frac{2l}{N}\pi, \frac{2(l+1)}{N}\pi\right)$, the cosine-term changes sign and the sine-term remains constant in sign. Therefore, the first-derivative of the partial sums changes its sign at every point $\frac{2l}{N}$, thus we get that these points are alternatively minima and maxima.

To conclude, for $1 \leq l \leq N$ the partial sum $S_N(x)$ has its relative maxima at $x = \frac{2l+1}{N+1}\pi$ and has its relative minima at $x = \frac{2l}{N}\pi$.

3.3.2. Behaviour in extreme points

In order to determine how S_N behaves at its first maximum $\left(\frac{\pi}{N+1}\right)$ and its first minimum $\left(\frac{2}{N}\pi\right)$ we consider several theorems. It is important to observe that these extreme points tend to zero as $N \to \infty$. Hence, the first maxima and minima become closer to zero as the number of Fourier terms increases.

We first show that the sequences $\left(S_N\left(\frac{2s-1}{N+1}\pi\right)\right)_{N=1}^{\infty}$ and $\left(S_N\left(\frac{2s}{N}\pi\right)\right)_{N=1}^{\infty}$ are ultimately increasing, for which we use the result of an additional theorem, stated in Appendix A.2.

Theorem 3.3. *For $0 \leq l \leq \left[\frac{1}{2}(N-1)\right]$, we have*

$$S_{N+1}\left(\frac{2l+1}{N+2}\pi\right) > S_N\left(\frac{2l+1}{N+1}\pi\right),$$

and for $1 \leq l \leq \left[\frac{1}{2}(N-1)\right]$ we have

$$S_{N+1}\left(\frac{2l}{N+1}\pi\right) > S_N\left(\frac{2l}{N}\pi\right).$$

Proof. It is trivial that $\frac{2l+1}{N+2}\pi < \frac{2l+1}{N+1}\pi < \frac{2l+2}{N+1}\pi$.
Now since S_{N+1} has a maximum at $\frac{2l+1}{N+2}\pi$ and its next minimum at $\frac{2l+2}{N+1}\pi$, we get the partial sums decreases in this interval.
Therefore we get

$$\begin{aligned} S_{N+1}\left(\frac{2l+1}{N+2}\pi\right) &> S_{N+1}\left(\frac{2l+1}{N+1}\pi\right) \\ &\overset{(1)}{=} S_N\left(\frac{2l+1}{N+1}\pi\right) + \frac{1}{N+1}\sin\left((N+1)\frac{2l+1}{N+1}\pi\right) \\ &= S_N\left(\frac{2l+1}{N+1}\pi\right) + \frac{1}{N+1}\sin\left((2l+1)\pi\right) \\ &\overset{(2)}{=} S_N\left(\frac{2l+1}{N+1}\pi\right). \end{aligned}$$

In the first step we write the S_{N+1} in terms of S_N and its final term. Step (2) follows from the fact that $\sin(k\pi) = 0$ for all $k \in \mathbb{Z}$.

□

Now, we are able to prove the main result of this section which shows that the values of the partial sums at the extreme points converge to limit numbers related to the sine integral function.

Theorem 3.4. *For every $s \in \mathbb{Z}_{>0}$, the sequence $\left(S_N\left(\frac{2s-1}{N+1}\pi\right)\right)_{N=1}^{\infty}$ is ultimately increasing and has $\int_0^{(2s-1)\pi}\frac{\sin(t)}{t}dt$ as limit number and $\left(S_N\left(\frac{2s}{N}\pi\right)\right)_{N=1}^{\infty}$ is ultimately increasing and has $\int_0^{2s\pi}\frac{\sin(t)}{t}dt$ as limit number.*

Proof. First, we will consider the sequence $\left(S_N\left(\frac{2s-1}{n+1}\pi\right)\right)_{N=1}^{\infty}$.

$$\begin{aligned} S_N\left(\frac{2s-1}{N+1}\pi\right) &\overset{(Thm3.3)}{=} \sum_{k=1}^{N}\frac{1}{k}\sin\left(\frac{k(2s-1)}{N+1}\pi\right) \\ &= \sum_{k=1}^{N}\frac{1}{k}\sin\left(\frac{k(2s-1)}{N+1}\pi\right)\frac{\left(\frac{2s-1}{N+1}\pi\right)}{\left(\frac{2s-1}{N+1}\pi\right)} \\ &\overset{(*)}{=} \sum_{k=1}^{N}\left[\frac{1}{\frac{k(2s-1)}{N+1}\pi}\sin\left(\frac{k(2s-1)}{N+1}\pi\right)\right]\frac{2s-1}{N+1}\pi. \end{aligned}$$

Consider the interval $[0,(2s-1)\pi]$ and divide this interval into equally spaced sub-intervals starting from $\left[0,\frac{2s-1}{2}\pi\right)$ till the last sub-interval $\left(\frac{N(2s-1)}{N+1}\pi,(2s-1)\pi\right]$. Hence, we get $(N+1)$ sub-intervals of length $\frac{2s-1}{N+1}\pi$.
The Riemann sum is defined as the sum of the $(N+1)$ rectangles below the graph of the integrand. Thus, the equation between brackets in step (*) can be seen as a Riemann sum for the integral $\int_0^{(2s-1)\pi}\frac{\sin t}{t}dt$ for $t=\frac{k(2s-1)}{N+1}\pi$.
Now if we consider the limit $N\to\infty$, the length of the sub-intervals tend to zero from which we know that the Riemann sum converges to the actual integral.

Therefore we get the following expression in the limit

$$\lim_{N\to\infty} S_N\left(\frac{2s-1}{N+1}\pi\right)=\int_0^{(2s-1)\pi}\frac{\sin t}{t}dt. \tag{3.9}$$

Similar argument can be used for the sequence $\left(S_N\left(\frac{2s}{N}\pi\right)\right)_{N=1}^{\infty}$ to obtain

$$\lim_{N\to\infty} S_N\left(\frac{2s}{N}\pi\right)=\int_0^{2s\pi}\frac{\sin t}{t}dt. \tag{3.10}$$

□

To conclude, as we consider the partial sum in the limit $N\to\infty$ we get that the partial sum evaluated in the first maximum converges to the limit number $\int_0^{(2s-1)\pi}\frac{\sin t}{t}dt$ and the partial sum evaluated in the first minimum converges to the limit number $\int_0^{2s\pi}\frac{\sin t}{t}dt$.

The observation that the partial sum converges to a value independent of the number of terms used in the Fourier series illustrates that this behaviour doesn't vanish if we increase the amount of terms used in the expansion, see Figures 3.3 and 3.4. The Python code for these figures can be found in Appendix A.3.

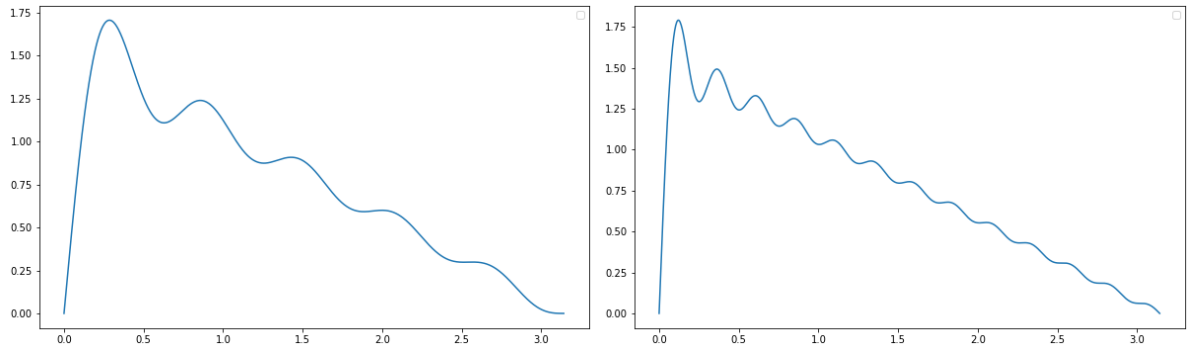

(a) Fourier series representation with $N=10$.

(b) Fourier series representation with $N=25$.

Figure 3.3: Fourier series representations.

3.3.3. Computing the amount of overshoot and undershoot near discontinuities

If we look at the first maximum, $\frac{\pi}{N+1}$, we obtain

$$\lim_{N\to\infty} S_N\left(\frac{\pi}{N+1}\right) = \text{Si}(\pi) = 1.8519370 = 1.1789797\left(\frac{1}{2}\pi\right). \tag{3.11}$$

As we consider the limit $N \to \infty$, the first maximum will tend to zero and the partial sums converge to the limit number $\text{Si}(\pi)$. Thus, the sum overshoots the line $\frac{1}{2}(\pi - x)$ by a factor of 1.1789797.
Considering the first minimum, $\frac{2}{N}\pi$, we obtain

$$\lim_{N\to\infty} S_N\left(\frac{2}{N}\pi\right) = \text{Si}(2\pi) = 1.4181516 = 0.9028233\left(\frac{1}{2}\pi\right). \tag{3.12}$$

Again, since we consider the limit $N \to \infty$, the first minimum will tend to zero and the partial sums converge to the limit number $\text{Si}(2\pi)$. Hence, the sum undershoots at the first minimum by a factor of 0.9028233. This is an example of the so-called Gibbs phenomenon for complex Fourier series of the function $f(x) = \frac{1}{2}(\pi - x)$ for $0 < x < 2\pi$ and can be seen in Figure 3.4.
To conclude, the behaviour of $S_N(x)$ near jump discontinuities is more complicated than just an overshoot in the convergence of the partial sum near the “jumps”.

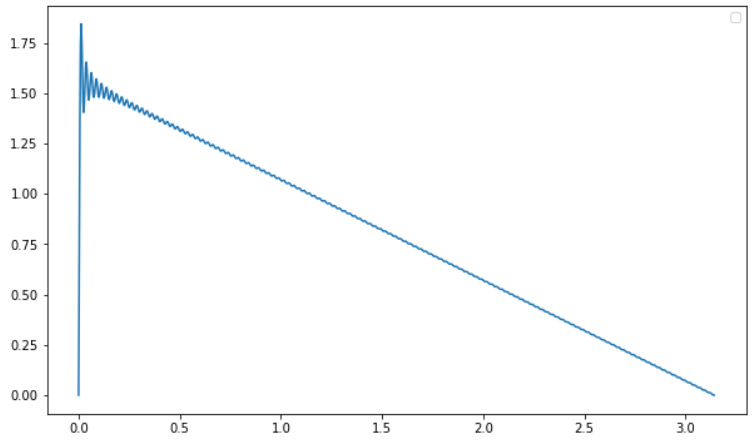

Figure 3.4: Fourier series representation of Saw-tooth wave function with $N = 250$.

The point where the maximum oscillation takes place will tend closer to the “jump”, in this case the value zero. Moreover, it is important to understand that the Gibbs phenomenon is not a contradiction of Theorem 2.2. Since in Theorem 2.2 we fix a certain point of discontinuity x and then consider the partial sum $S_N(x)$ in the limit $N \to \infty$. But in this chapter we considered the case where the point x was the first maximum or minimum that is dependent on N and tends to zero in the limit. However, the maximal oscillation itself does not vanish when more terms of the series are added. On the contrary, it stabilizes towards a value that is approximately 9% of the total height of the “jump”.

In the next chapter, we will see that the Gibbs phenomenon occurs in general for functions with jump discontinuities at arbitrary points.

4

General case

In this chapter, the result of Chapter 3 will be used in order to show the existence of the Gibbs phenomenon for simple functions with a jump discontinuity. In Subsection 4.1.1 we will show that the Gibbs phenomenon occurs when we consider a function with a jump discontinuity at the origin. Finally, we will extend this proof in Subsection 4.1.2 in order to show that functions with a finite number of jump discontinuities also exhibit the Gibbs phenomenon near the jump discontinuities.

4.1. Generalization of the Gibbs phenomenon

In order to prove the existence of the Gibbs phenomenon for a "general" function with a jump discontinuity at the origin, we first need to look at the uniform version of the Riemann-Lebesgue Lemma.

Theorem 4.1. *Suppose* $f \in L^1[-\pi,\pi]$ *is a periodic function and* $h \in C^1[\alpha,\beta]$ *such that* $[\alpha,\beta] \in [-\pi,\pi]$. *Then*

$$\int_\alpha^\beta f(x-u)h(u)\sin(\lambda u)du \to 0 \quad \textit{as} \quad \lambda \to \infty$$

uniformly in x.

Proof. We start the proof with using the fact that $C^1[-\pi,\pi]$ is dense in $L^1[-\pi,\pi]$. This means we can find a function $g \in C^1[-\pi,\pi]$ that is close to f in the L^1-norm. In other words, for all $\epsilon > 0$

$$||f-g||_{L^1} = \int_{-\pi}^{\pi} |f(x)-g(x)|dx < \epsilon.$$

Now consider the integral I to be

$$I = \int_\alpha^\beta g(x-u)h(u)\sin(\lambda u)du. \tag{4.1}$$

If we perform integration by parts we get

$$\begin{aligned} I &= g(x-u)h(u)\cdot -\frac{1}{\lambda}\cos(\lambda u)\Big|_{u=\alpha}^{u=\beta} - \int_\alpha^\beta \frac{d}{du}\left[g(x-u)h(u)\right]\cdot -\frac{1}{\lambda}\cos(\lambda u)du \\ &= -g(x-u)h(u)\frac{\cos(\lambda u)}{\lambda}\Big|_{u=\alpha}^{u=\beta} + \int_\alpha^\beta \frac{d}{du}\left[g(x-u)h(u)\right]\frac{\cos(\lambda u)}{\lambda}du. \end{aligned}$$

Since $-g(x-u)h(u)$ and $\frac{d}{du}\left[g(x-u)h(u)\right]$ are both uniformly bounded and $\frac{\cos(\lambda u)}{\lambda}$ tends to zero as $\lambda \to \infty$, we get that I converges uniformly to zero as λ tends to ∞.

Thus,let $\epsilon > 0$ arbitrary, if we consider the absolute value of the integral

$$\int_\alpha^\beta f(x-u)h(u)\sin(\lambda u)du$$

and use the previous result, we obtain

$$\begin{aligned}\left|\int_\alpha^\beta f(x-u)h(u)\sin(\lambda u)du\right| &\le \left|\int_\alpha^\beta \left[f(x-u)-g(x-u)\right]h(u)\sin(\lambda u)du\right| + \left|\int_\alpha^\beta g(x-u)h(u)\sin(\lambda u)du\right| \\ &= \left|\int_\alpha^\beta \left[f(x-u)-g(x-u)\right]h(u)\sin(\lambda u)du\right| + |I| \\ &\le \max_{\alpha\le u\le\beta}|h(u)|\int_\alpha^\beta \left|\left[f(x-u)-g(x-u)\right]\right|du + |I| \\ &\le \max_{\alpha\le u\le\beta}|h(u)|\epsilon + |I|.\end{aligned}$$

To conclude, as $\lambda\to\infty$ we get I goes to zero and we obtain the desired result. □

Furthermore, we need Theorem 4.2 about the convergence of the partial Fourier sum of an α-Hölder continuous function.

Theorem 4.2. *Let f be a function such that the left- and right-hand limit $f(x_0^+)$, $f(x_0^-)$ satisfy the α-Hölder continuity condition at x_0. Then*

$$\lim_{n\to\infty} S_N[f](x_0) = \frac{f(x_0^+)+f(x_0^-)}{2}.$$

Proof. In this proof we will consider the case $x_0\neq\pm\pi$. For the case $x_0=\pm\pi$, a translation by π and then using the same argument will give $S_N[f](x-\pi)\to\bar{f}(x-\pi)$ at $x=0$.
By using the properties of the Dirichlet kernel, stated in Theorem 2.1, we obtain the following equation

$$S_N[f](x)-f(x) = \frac{1}{2\pi}\int_{-\pi}^{\pi}\left[f(x-u)-f(x)\right]D_N(u)du. \tag{4.2}$$

Now define

$$\bar{f}(x_0) = \frac{f(x_0^+)+f(x_0^-)}{2} \tag{4.3}$$

and insert this expression in (4.2) to get

$$S_N[f](x_0)-\bar{f}(x_0) = \frac{1}{2\pi}\int_{-\pi}^{\pi}\left[f(x_0-u)-\bar{f}(x_0)\right]D_N(u)du.$$

Substituting (4.3) will give

$$\begin{aligned}S_N[f](x_0)-\bar{f}(x_0) &= \frac{1}{2\pi}\int_{-\pi}^{\pi}\left[f(x_0-u)-\left(\frac{f(x_0^+)+f(x_0^-)}{2}\right)\right]D_N(u)du \\ &= \frac{1}{2\pi}\int_{-\pi}^{\pi}\left[f(x_0-u)-\frac{f(x_0^+)}{2}-\frac{f(x_0^-)}{2}\right]D_N(u)du.\end{aligned} \tag{4.4}$$

Then, we use linearity of the integral and split the integration interval $[-\pi,\pi]$ into sub-intervals to get the following integrals

$$\begin{aligned}S_N[f](x_0)-\bar{f}(x_0) &= \frac{1}{2\pi}\int_0^\pi f(x_0-u)D_N(u)du - \frac{1}{2\pi}\int_0^\pi\frac{f(x_0^+)}{2}D_N(u)du - \frac{1}{2\pi}\int_0^\pi\frac{f(x_0^-)}{2}D_N(u)du \\ &+ \frac{1}{2\pi}\int_{-\pi}^0 f(x_0-u)D_N(u)du - \frac{1}{2\pi}\int_{-\pi}^0\frac{f(x_0^+)}{2}D_N(u)du - \frac{1}{2\pi}\int_{-\pi}^0\frac{f(x_0^-)}{2}D_N(u)du \\ &= \frac{1}{2\pi}\int_0^\pi\left(f(x_0-u)-f(x_0^-)\right)D_N(u)du + \frac{1}{2\pi}\int_0^\pi\frac{f(x_0^-)}{2}D_N(u)du \\ &- \frac{1}{2\pi}\int_0^\pi\frac{f(x_0^+)}{2}D_N(u)du + \frac{1}{2\pi}\int_{-\pi}^0\left(f(x_0-u)-f(x_0^+)\right)D_N(u)du \\ &+ \frac{1}{2\pi}\int_{-\pi}^0\frac{f(x_0^+)}{2}D_N(u)du - \frac{1}{2\pi}\int_{-\pi}^0\frac{f(x_0^-)}{2}D_N(u)du \\ &= I_1+I_2+I_3+I_4+I_5+I_6.\end{aligned}$$

Now we will rewrite $I_5 + I_6$ by using the fact that the Dirichlet kernel is an even function and applying a change of variables with $y = -u$.

$$\begin{aligned} I_5 + I_6 &= \frac{1}{2\pi}\int_{-\pi}^{0} \frac{f(x_0^+)}{2} D_N(u)du - \frac{1}{2\pi}\int_{-\pi}^{0} \frac{f(x_0^-)}{2} D_N(u)du \\ &= \frac{1}{2\pi}\int_{-\pi}^{0} \frac{f(x_0^+)}{2} D_N(-y)(-dy) - \frac{1}{2\pi}\int_{-\pi}^{0} \frac{f(x_0^-)}{2} D_N(-y)(-dy) \\ &= -\frac{1}{2\pi}\int_{-\pi}^{0} \frac{f(x_0^+)}{2} D_N(y)dy + \frac{1}{2\pi}\int_{-\pi}^{0} \frac{f(x_0^-)}{2} D_N(y)dy \\ &= \frac{1}{2\pi}\int_{0}^{\pi} \frac{f(x_0^+)}{2} D_N(y)dy - \frac{1}{2\pi}\int_{0}^{\pi} \frac{f(x_0^-)}{2} D_N(y)dy \\ &= -(I_2 + I_3), \end{aligned}$$

thus we get $I_2 + I_3 + I_5 + I_6 = 0$. Therefore, we obtain

$$\begin{aligned} S_N[f](x_0) - \bar{f}(x_0) &= I_1 + I_4 \\ &= \frac{1}{2\pi}\int_{0}^{\pi} \left(f(x_0 - u) - f(x_0^-)\right) D_N(u)du + \frac{1}{2\pi}\int_{-\pi}^{0} \left(f(x_0 - u) - f(x_0^+)\right) D_N(u)du. \end{aligned}$$

Let $0 < \delta < \pi$. In step (1) we split the integration interval and in step (2) we divide and multiply by u to obtain

$$\begin{aligned} S_N[f](x_0) - \bar{f}(x_0) &\overset{(1)}{=} \frac{1}{2\pi}\int_{-\pi}^{-\delta} \left(f(x_0 - u) - f(x_0^+)\right) D_N(u)du + \frac{1}{2\pi}\int_{-\delta}^{0} \left(f(x_0 - u) - f(x_0^+)\right) D_N(u)du \\ &+ \frac{1}{2\pi}\int_{0}^{\delta} \left(f(x_0 - u) - f(x_0^-)\right) D_N(u)du + \frac{1}{2\pi}\int_{\delta}^{\pi} \left(f(x_0 - u) - f(x_0^-)\right) D_N(u)du \\ &\overset{(2)}{=} \frac{1}{2\pi}\int_{-\pi}^{-\delta} \left(\frac{f(x_0 - u) - f(x_0^+)}{u}\right) uD_N(u)du + \frac{1}{2\pi}\int_{-\delta}^{0} \left(\frac{f(x_0 - u) - f(x_0^+)}{u}\right) uD_N(u)du \\ &+ \frac{1}{2\pi}\int_{0}^{\delta} \left(\frac{f(x_0 - u) - f(x_0^-)}{u}\right) uD_N(u)du + \frac{1}{2\pi}\int_{\delta}^{\pi} \left(\frac{f(x_0 - u) - f(x_0^-)}{u}\right) uD_N(u)du \\ &= J_1 + J_2 + J_3 + J_4. \end{aligned}$$

Now it suffices to show that given $\epsilon > 0$, there exist $\delta > 0$ and $N' \in \mathbb{N}$ such that these choices imply that for all $N \geq N'$ we get $|S_N[f](x_0) - \bar{f}(x_0)| = |J_1 + J_2 + J_3 + J_4| < \epsilon$.

For integrals J_1 and J_4 we use the expression of the Dirichlet kernel from (2.5) to rewrite them in terms of Fourier coefficients and then apply the Riemann Lebesgue Lemma to obtain $|J_1| + |J_4| \leq \frac{\epsilon}{2}$.

$$
\begin{aligned}
J_1 &= \frac{1}{2\pi}\int_{-\pi}^{-\delta}\left(\frac{f(x_0-u)-f(x_0^+)}{u}\right)uD_N(u)du \\
&= \frac{1}{2\pi}\int_{-\pi}^{-\delta}\left(f(x_0-u)-f(x_0^+)\right)\frac{\sin\left(N+\frac{1}{2}\right)u}{\sin\left(\frac{u}{2}\right)}du \\
&= \frac{1}{2\pi}\int_{-\pi}^{-\delta}\left(f(x_0-u)-f(x_0^+)\right)\frac{1}{\sin\left(\frac{u}{2}\right)}\left(\sin(Nu)\cos\left(\frac{u}{2}\right)+\cos(Nu)\sin\left(\frac{u}{2}\right)\right)du \\
&= \frac{1}{2\pi}\int_{-\pi}^{-\delta}\left(f(x_0-u)-f(x_0^+)\frac{\cos\left(\frac{u}{2}\right)}{\sin\left(\frac{u}{2}\right)}\right)\sin(Nu)du+\frac{1}{2\pi}\int_{-\pi}^{-\delta}\left(f(x_0-u)-f(x_0^+)\right)\cos(Nu)du \\
&= \frac{1}{2\pi}\int_{-\pi}^{\pi}\left(f(x_0-u)-f(x_0^+)\frac{\cos\left(\frac{u}{2}\right)}{\sin\left(\frac{u}{2}\right)}\chi_{[-\pi,-\delta]}(u)\right)\sin(Nu)du \\
&+ \frac{1}{2\pi}\int_{-\pi}^{\pi}\left(f(x_0-u)-f(x_0^+)\chi_{[-\pi,-\delta]}(u)\right)\cos(Nu)du \\
&= \frac{1}{2\pi}\int_{-\pi}^{\pi}g(x_0,u)\sin(Nu)du+\frac{1}{2\pi}\int_{-\pi}^{\pi}h(x_0,u)\cos(Nu)du \\
&= A+B.
\end{aligned}
$$

Since $f\in L^1(\pi,\pi)$ and $\sin\left(\frac{u}{2}\right)$ is bounded in the interval $[-\pi,-\delta]$, we get both g and h are in $L^1(\pi,\pi)$ and the integrals A and B are the Fourier coefficients of g and h. Therefore, by the Riemann Lebesgue Lemma we get that A and B tend to zero as $N\to\infty$. Hence, $J_1\to 0$ as $N\to\infty$. Similar argument can be used in order to show $J_4\to 0$ as $N\to\infty$. Thus we can choose $\delta>0$ and $N'\in\mathbb{N}$ such that $|J_1|+|J_4|\le\frac{\epsilon}{2}$.

As for the other two integrals, we use the α-Hölder continuity condition to show $|J_2|+|J_3|\le\frac{\epsilon}{2}$.

$$
\begin{aligned}
|J_2| &= \frac{1}{2\pi}\left|\int_{-\delta}^{0}\left(\frac{f(x_0-u)-f(x_0^+)}{u}\right)uD_N(u)du\right| \\
&= \frac{1}{2\pi}\left|\int_{-\delta}^{0}\left(\frac{f(x_0-u)-f(x_0^+)}{u}\right)\frac{u}{\sin\left(\frac{u}{2}\right)}\sin\left(\left(N+\frac{1}{2}\right)u\right)du\right| \\
&\le \frac{1}{2\pi}\int_{-\delta}^{0}\left|\left(\frac{f(x_0-u)-f(x_0^+)}{u}\right)\frac{u}{\sin\left(\frac{u}{2}\right)}\sin\left(\left(N+\frac{1}{2}\right)u\right)\right|du
\end{aligned}
$$

By the α-Hölder continuity condition on $f(x)$ we know that

$$|f(x)-f(x_0)|\le M_1|x-x_0|^\alpha,\quad \text{if}\quad |x-x_0|<\delta.$$

Therefore, $|f(x_0-u)-f(x_0)|\le M_1|x_0-u-x_0|^\alpha=M_1|u|^\alpha$.

Since we have $|\sin\left(\left(N+\frac{1}{2}\right)u\right)|\le 1$, let $|u|<\delta$ to get $\left|\frac{u}{\sin\left(\frac{u}{2}\right)}\right|\le M_3$.

Combining these bounds we obtain

$$|J_2|\le M_3\int_{-\delta}^{0}M_1|u|^{\alpha-1}du\le M\int_{-\delta}^{0}|u|^{\alpha-1}du. \tag{4.5}$$

Similarly, we obtain

$$|J_3|\le M_3\int_{0}^{\delta}M_2|u|^{\alpha-1}du\le M\int_{0}^{\delta}|u|^{\alpha-1}du, \tag{4.6}$$

where $M=\max\{M_3M_1,M_3M_2\}$.

Hence, we get

$$\begin{aligned} |J_2| + |J_3| &\leq M \int_{-\delta}^{0} |u|^{\alpha-1} du + M \int_{0}^{\delta} |u|^{\alpha-1} du \\ &\leq \frac{M}{2} \int_{-\delta}^{0} |u|^{\alpha-1} du + \frac{M}{2} \int_{0}^{\delta} |u|^{\alpha-1} du \\ &= \frac{M}{2} \int_{-\delta}^{\delta} |u|^{\alpha-1} du \\ &= M \int_{0}^{\delta} |u|^{\alpha-1} du \\ &= M \frac{|u|^{\alpha}}{\alpha} \Big|_{0}^{\delta} \\ &= \frac{M}{\alpha} \delta^{\alpha}. \end{aligned} \tag{4.7}$$

To conclude, given $\epsilon > 0$, we can choose $\delta > 0$ and $N' \in \mathbb{N}$ such that for all $N \geq N'$ we get $|S_N[f](x_0) - \tilde{f}(x_0)| < \epsilon$. □

In order to show uniform convergence we need the uniform Riemann Lebesgue Lemma, stated in Theorem 4.1, and the following theorem.

Theorem 4.3. *Suppose f satisfies the uniform α-Hölder continuity condition of order $0 < \alpha \leq 1$ in (a, b). Then $S_N[f] \to f$ uniformly in any interior subinterval $[c, d] \subset (a, b)$.*

Proof. Let $\delta < \min(c - a, b - d)$. From (4.7) of the previous proof we get $|J_2| + |J_3| \leq \frac{M}{\alpha}\delta^{\alpha}$.
Now write J_1 as

$$\begin{aligned} J_1 &= \frac{1}{2\pi} \int_{-\pi}^{-\delta} \left(f(x_0 - u) - f(x_0^+)\right) \frac{\sin\left(\left(N + \frac{1}{2}\right) u\right)}{\sin\left(\frac{u}{2}\right)} du \\ &= \frac{1}{2\pi} \int_{-\pi}^{-\delta} f(x_0 - u) \frac{\sin\left(\left(N + \frac{1}{2}\right) u\right)}{\sin\left(\frac{u}{2}\right)} du - \frac{1}{2\pi} \int_{-\pi}^{-\delta} f(x_0^+) \frac{\sin\left(\left(N + \frac{1}{2}\right) u\right)}{\sin\left(\frac{u}{2}\right)} du. \end{aligned}$$

Since $\frac{1}{\sin\left(\frac{u}{2}\right)} \in C^1[-\pi, -\delta]$ we can apply the uniform Riemann Lebesgue Lemma with $\alpha = -\pi$, $\beta = -\delta$ and $\lambda = N + \frac{1}{2}$ to get uniform convergence to zero of J_1 as $N \to \infty$. According to the same argument we get J_4 converges uniformly to zero as $N \to \infty$. □

These convergence results enable us to show that a "general" function g with a jump discontinuity at the origin exhibits the Gibbs phenomenon. Because it is now sufficient to show the occurrence of the phenomenon for another simple function (such as the Saw-tooth wave function), in order to conclude that g also shows this behavior near the origin. To elaborate this result, we consider the following example.

4.1.1. Jump discontinuity at 0

Suppose $g(x)$ is a piecewise smooth function with a jump at 0 such that the left- and right-limits $g(0^+)$ and $g(0^-)$ both exist and are finite.
In order to "remove" the discontinuity at 0 we consider the function $h(x)$ defined as

$$h(x) = g(x) - \left(\frac{g(0^+) - g(0^-)}{\pi}\right) f(x), \tag{4.8}$$

where f is the Saw-tooth wave function investigated in Chapter 3.

Now look at the limits as $x \to 0^+$ and as $x \to 0^-$.

$$\lim_{x\to 0^+} h(x) = g(0^+) - \left(\frac{g(0^+) - g(0^-)}{\pi}\right)\frac{\pi}{2} = \frac{g(0^+) - g(0^-)}{2}$$

and

$$\lim_{x\to 0^-} h(x) = g(0^-) - \left(\frac{g(0^+) - g(0^-)}{\pi}\right)\left(-\frac{\pi}{2}\right) = \frac{g(0^+) - g(0^-)}{2}.$$

Define

$$h(0) := \frac{g(0^+) - g(0^-)}{2},$$

then $h(x)$ is continuous at 0, since both left- and right-hand limits exist finite and are equal. Therefore, the function $h(x)$ satisfies the hypothesis of Theorem 4.2, so we get $S_N[h](x)$ converges at 0. Moreover, by Theorem 4.3 we have uniform convergence in a neighborhood of 0. Therefore, we can conclude that since f exhibits the Gibbs phenomenon near 0, it must also holds for the function g.

4.1.2. Jump discontinuity at general point

Consider a function g with a jump discontinuity at a general point $x = x_0$ and that is piecewise smooth everywhere else. Then we can define the function

$$h(x) = \begin{cases} g(x) - \left(\frac{g(x_0^+) - g(x_0^-)}{\pi}\right) f(x - x_0) & \text{if} \quad x \neq x_0 \\ \frac{g(x_0^+) - g(x_0^-)}{2} & \text{if} \quad x = x_0 \end{cases}, \tag{4.9}$$

in which $f(x-x_0)$ is a function known to exhibit the Gibbs phenomenon. Then, we get that the left-hand limit is equal to the right-hand limit, so we get

$$\lim_{x\to x_0^+} h(x) = \lim_{x\to x_0^-} h(x) = h(x_0) = \frac{g(x_0^+) - g(x_0^-)}{2}.$$

Hence, h is continuous at $x = x_0$ and therefore by Theorem 4.2, the partial sum $S_N[h]$ converges uniformly near x_0. Since the Gibbs phenomenon occurs in $f(x-x_0)$, we conclude from the convergence results in Subsection 4.1.1 that $g(x)$ displays the Gibbs phenomenon as well at $x = x_0$.

We can use the same argument for finitely many points $x_1, ..., x_j$ for which $g(x)$ has a jump discontinuity by defining the function

$$\hat{h}(x) = \begin{cases} g(x) - \left(\frac{\sum_j g(x_j^+) - g(x_j^-)}{\pi}\right) f(x - x_0) & \text{if} \quad x \neq x_j \\ \frac{g(x_j^+) - g(x_j^-)}{2} & \text{if} \quad x = x_j \end{cases}. \tag{4.10}$$

5

Resolution Gibbs phenomenon

Using Fourier series expansions for approximating functions has proved to be a powerful technique for simulations of several physical phenomena. However, as we have seen in previous chapters, the Gibbs phenomenon arises when we approximate a function with a jump discontinuity. Specifically, the convergence of the Fourier coefficients to zero deteriorates to the first-order and spurious oscillations develop near the jump discontinuities. The problems that characterize the Gibbs phenomenon are also present in Fourier spectral methods applied to partial differential equations with discontinuous functions [8].

In this chapter we present techniques that can significantly reduce the effects of the Gibbs phenomenon. In Section 5.1 we elaborate the problem of the slow convergence rate of the Fourier coefficients in more detail. In Section 5.2 we review the use of filters in Fourier expansions of functions with jump discontinuities. However, filtering does not completely remove the Gibbs phenomenon. In order to completely remove the Gibbs phenomenon, one can use spectral reprojection methods. The general idea of these reprojection methods is that we can reconstruct a rapidly converging series from the knowledge of the Fourier coefficients by using different expansion functions. Thus the storage of the information (in Fourier coefficients) remains the same, but the retrieval of the information should be done in a different basis. This method was first introduced in [6] and will be explained in more detail in Section 5.3.

5.1. Convergence rate

One of the manifestations of the Gibbs phenomenon is that the Fourier coefficients decay slowly. This can be explained by the global nature of the approximation: the Fourier coefficients of a 2π-periodic, piecewise continuous function f with jump discontinuities in the interval $[-\pi, \pi]$ are computed by

$$\hat{f}(n) = \frac{1}{2\pi} \int_{-\pi}^{\pi} f(t) e^{-int} dt. \tag{5.1}$$

Hence, they are obtained by integration over the entire domain, including the points of discontinuity.

In the following theorem it becomes clear that we get first-order convergence of the Fourier coefficients when we consider 2π-periodic piecewise continuous functions.

Theorem 5.1. *Let f be 2π-periodic and piecewise continuous, then*

$$\hat{f}(n) = \mathcal{O}\left(\frac{1}{|n|}\right), \quad |n| \to \infty.$$

Proof. Let $a_0 = -\pi < a_1 < a_2 < ... < a_m = \pi$ be a partition of $[-\pi, \pi]$ such that f is piecewise continuous on (a_j, a_{j+1}) and the left- and right-hand limits exist finite for all $j = 0, ..., m-1$.
Let $n \in \mathbb{Z}$, $n \neq 0$. Then we get

$$\hat{f}(n) = \frac{1}{2\pi} \int_{-\pi}^{\pi} f(t) e^{-int} dt = \frac{1}{2\pi} \sum_{j=0}^{m-1} \int_{a_j}^{a_{j+1}} f(t) e^{-int} dt. \tag{5.2}$$

Now consider f on a certain interval $[a_j, a_{j+1}]$ for $0 \leq j \leq n-1$. Define $\tilde{f}_j : [a_j, a_{j+1}] \to \mathbb{C}$ as

$$\tilde{f}_j(t) = \begin{cases} f(t) & \text{for} \quad a_j < t < a_{j+1} \\ \lim_{t \to a_j^+} f(t) & \text{for} \quad t = a_j \\ \lim_{t \to a_{j+1}^-} f(t) & \text{for} \quad t = a_{j+1} \end{cases}, \tag{5.3}$$

then $\tilde{f}_j$ is a continuous function on $[a_j, a_{j+1}]$. Therefore, by using integration by parts we get

$$\begin{aligned} \int_{a_j}^{a_{j+1}} f(t) e^{-int} dt &= \int_{a_j}^{a_{j+1}} \tilde{f}_j(t) e^{-int} dt \\ &= -\frac{1}{in} \tilde{f}_j(t) e^{-int} \Big|_{t=a_j}^{t=a_{j+1}} + \frac{1}{in} \int_{a_j}^{a_{j+1}} \tilde{f}_j'(t) e^{-int} dt \\ &= -\frac{1}{in} \left[\tilde{f}_j(a_{j+1}) e^{-ina_{j+1}} - \tilde{f}_j(a_j) e^{-ina_j} \right] + \frac{1}{in} \int_{a_j}^{a_{j+1}} \tilde{f}_j'(t) e^{-int} dt \\ &= \frac{1}{in} \int_{a_j}^{a_{j+1}} f'(t) e^{-int} dt - \frac{1}{in} \left[f(a_{j+1}^-) e^{-ina_{j+1}} - f(a_j^+) e^{-ina_j} \right]. \end{aligned} \tag{5.4}$$

If we look at the first part we get a finite integral and in the second part we get a constant. Thus, we can estimate this integral with

$$\left| \int_{a_j}^{a_{j+1}} f(t) e^{-int} dt \right| \leq \frac{1}{|n|} \int_{a_j}^{a_{j+1}} |f'(t)| dt + \frac{1}{|n|} \left(|f(a_{j+1}^-)| + |f(a_j^+)| \right). \tag{5.5}$$

Consequently, when we put these estimates together we obtain

$$|\hat{f}(n)| \leq \frac{1}{2\pi} \frac{1}{|n|} \int_{-\pi}^{\pi} |f'(t)| dt + \frac{1}{2\pi} \frac{1}{|n|} \sum_{j=0}^{m-1} \left(|f(a_{j+1}^-)| + |f(a_j^+)| \right). \tag{5.6}$$

Hence, we get $|\hat{f}(n)| \leq \frac{1}{|n|} \cdot C$, where C is a constant.
From this we can conclude that $|\hat{f}(n)| = \mathcal{O}\left(\frac{1}{|n|}\right)$ for $|n| \to \infty$ □

Thus we have first-order convergence of Fourier coefficients away from the jump discontinuity and non-uniform convergence (oscillating behaviour) near the jump discontinuity.

5.2. Filtering methods

Filtering is a classical tool for reducing the effect of the Gibbs phenomenon in Fourier expansions. By using a filter we alter the expansion coefficients so that they decay faster. While this will not improve the non-uniform convergence near the jump discontinuity, a well chosen filter can improve the convergence rate away from the jump discontinuity.

We define a filter of order q, where we use the notation as in [8].

Definition 5.1. A filter of order q is a real and even function $\sigma(\eta) \in C^{q-1}(\mathbb{R})$ with the following properties:

(a) $\sigma(\eta) = 0 \quad$ for $\quad |\eta| > 1$

(b) $\sigma(0) = 1, \quad \sigma(1) = 0$

(c) $\sigma^{(m)}(0) = \sigma^{(m)}(1) = 0 \quad$ for all $\quad m \in [1, ..., q-1]$.

Now assume the following situation: we are given the first $2N+1$ Fourier coefficients of a piecewise analytic function $f(x)$ that has a jump discontinuity at $x = \xi$. The classical approximation based on the Fourier expansion would be the Nth partial Fourier sum

$$S_N[f](x) = \sum_{k=-N}^{N} \hat{f}(k) e^{ikx}. \tag{5.7}$$

This partial Fourier sum approximation yields the Gibbs phenomenon, so first-order convergence away from the jump discontinuity at $x = \xi$ and oscillations near the jump discontinuity. To improve the convergence rate of (5.7), we use the filter $\sigma\left(\frac{|k|}{N}\right)$.
Applying a filter can be seen as modifying the classical Fourier sum (5.7) by multiplying the Fourier coefficients with a Fourier space filter such that we obtain the modified approximation

$$S_N^\sigma[f](x) = \sum_{k=-N}^{N} \sigma\left(\frac{|k|}{N}\right) \hat{f}(k) e^{ikx}. \tag{5.8}$$

Now, there are two important observations that can be made. First of all, it is crucial that the filtered approximation is a continuous function in order to improve the convergence rate.
Secondly, we can rewrite the filtered approximation (5.8) to an infinite sum by using the following property of the filter: $\sigma(\eta) = 0$ for $\eta = \frac{|k|}{N} \geq 1$. Hence, we obtain

$$S_N^\sigma[f](x) = \sum_{k=-\infty}^{\infty} \sigma\left(\frac{|k|}{N}\right) \hat{f}(k) e^{ikx}. \tag{5.9}$$

Since now the effect of truncating the amount of Fourier coefficients used is removed, the truncation error will vanish. This means that we have obtained a fast decay of the Fourier coefficients when we use a filtered approximation.

More formally, this can be seen as a convolution

$$S_N^\sigma[f](x) = \frac{1}{2\pi} \int_{-\pi}^{\pi} S(x-y) f(y) dy, \tag{5.10}$$

where the filter function is given by

$$S(z) = \sum_{k=-\infty}^{\infty} \sigma\left(\frac{|k|}{N}\right) e^{ikz}. \tag{5.11}$$

Proof. By direct computation, we get

$$\begin{aligned} S_N^\sigma[f](x) &= \frac{1}{2\pi}\int_{-\pi}^{\pi} S(x-y)f(y)dy \\ &= \frac{1}{2\pi}\int_{-\pi}^{\pi}\left[\sum_{k=-\infty}^{\infty}\sigma\left(\frac{|k|}{N}\right)e^{ik(x-y)}\right]f(y)dy \\ &= \sum_{k=-\infty}^{\infty}\sigma\left(\frac{|k|}{N}\right)\left[\frac{1}{2\pi}\int_{-\pi}^{\pi}e^{ik(x-y)}f(y)dy\right] \\ &= \sum_{k=-\infty}^{\infty}\sigma\left(\frac{|k|}{N}\right)\left[\frac{1}{2\pi}\int_{-\pi}^{\pi}e^{-iky}f(y)dy\right]e^{ikx} \\ &= \sum_{k=-\infty}^{\infty}\sigma\left(\frac{|k|}{N}\right)\hat{f}(k)e^{ikx}. \end{aligned} \tag{5.12}$$

□

Since $f(x)$ is a piecewise $C^p(\mathbb{R})$ function with a single jump discontinuity at $x = \xi$, we get that the following theorem holds.

Theorem 5.2. *The pointwise difference between the filtered approximation f_N^σ and the function $f(x)$ away from the discontinuity (so $x \neq \xi$) is bounded by*

$$|f(x) - S_N^\sigma[f](x)| \leq C_1\frac{1}{N^{p-1}}\frac{1}{d(x)^{p-1}}K(f) + C_2\frac{\sqrt{N}}{N^p}\left(\int_{-\pi}^{\pi}|f^{(p)}|^2dx\right)^{\frac{1}{2}}, \tag{5.13}$$

where $d(x) = |x - \xi|$ is defined as the distance between a point $x \in [-\pi, \pi]$ and the discontinuity, and

$$K(f) = \sum_{l=0}^{p-1} d(x)^l|f^{(l)}(\xi^+) - f^{(l)}(\xi^-)|\int_{-\infty}^{\infty}|G_l^{(p-l)}(\eta)|d\eta$$

with

$$G_l(\eta) = \frac{\sigma(\eta) - 1}{\eta^l}.$$

This bound is obtained by estimating the truncation error and regularization error of the approximation and the detailed formal proof can be found in [6].

To conclude, filtering improves the convergence rate away from the discontinuity ($d(x) > 0$), since all terms can be bounded by $\mathcal{O}(N^{1-p})$ depending only on the regularity of the piecewise continuous function and the order of the filter. However, when we approach the discontinuity at $x = \xi$, the accuracy of the approximation decreases as $d(x) \to 0$ and thus it fails to completely remove the Gibbs phenomenon.

5.3. Spectral reprojection methods

If the underlying function is piecewise analytic, the Gibbs phenomenon can be completely removed by re-expanding its Fourier partial sum approximation (5.7) using a different set of basis functions.

In this section we will show that this is indeed true for a function $f(x) \in L^2[-1,1]$ that is analytic on some subinterval $[a,b] \subset [-1,1]$.
Let $\{\Psi_k(x)\}$ be an orthonormal family under some inner product $(\cdot,\cdot)$. Assume that the inner product is bounded $|(f,\Psi_k)| \leq C$ by some constant C independent of k. Furthermore, denote the finite continuous expansion in this orthonormal basis by

$$\tilde{f}_N(x) = \sum_{k=0}^{N} (f,\Psi_k)\Psi_k(x) \tag{5.14}$$

and assume this is a good approximation of the function $f(x)$ almost everywhere. Thus

$$\lim_{N\to\infty} |f(x) - \tilde{f}_N(x)| = 0, \tag{5.15}$$

almost everywhere in $x \in [-1,1]$.

Due to the global nature of the expansion, the fact that the coefficients are computed over the entire domain, the approximation inside the analytic sub-interval $[a,b]$ converges slowly if there is any jump discontinuity outside this interval.
However, under certain conditions we will show that it is possible to get a higher order approximation of $f(x)$ in the interval $[a,b]$. This can be done by re-expanding $\tilde{f}_N(x)$ in a so-called "Gibbs complementary family" basis.

First of all, we use the linear transformation of $x \in [a,b]$ to $\xi \in [-1,1]$.

$$\xi = -1 + 2\left(\frac{x-a}{b-a}\right),$$

such that if $a \leq x \leq b$, then $-1 \leq \xi \leq 1$.

Now, consider the re-expansion of $\tilde{f}_N(x)$ by using a different orthonormal family of functions $\{\phi_k^\lambda\}$ defined in an interval $[a,b]$ that is analytic and some inner product $<,>_\lambda$.

$$f_m^\lambda(x) = \sum_{k=0}^{m} < \tilde{f}_N(x), \phi_k^\lambda >_\lambda \phi_k^\lambda(\xi(x)), \tag{5.16}$$

where the family $\{\phi_k^\lambda\}$ is orthonormal under the inner product $<,>_\lambda$. Then this new expansion $f_m^\lambda(x)$ converges exponentially fast in the interval $[a,b]$ if the family $\{\phi_k^\lambda\}$ is *Gibbs complementary* to the family $\{\Psi_k(x)\}$. Where we consider the definition of Gibbs complementary from [8].

Definition 5.2. The family $\{\phi_k^\lambda\}$ is Gibbs complementary to the family $\{\Psi_k(x)\}$ if the following three conditions hold:

(i) **Orthonormality**

$$< \phi_k^\lambda(\xi), \phi_l^\lambda(\xi) >_\lambda = \delta_{kl}$$

for any fixed λ.

(ii) **Spectral convergence**
The expansion of a function $g(\xi)$ which is analytic in $-1 \leq \xi \leq 1$, in the basis $\phi_k^\lambda(\xi)$ converges exponentially fast with $\lambda = \beta m$ (λ proportional to N). In other words,

$$\max_{-1\leq\xi\leq 1} \left| g(\xi) - \sum_{k=0}^{m} < g, \phi_k^\lambda >_\lambda \phi_k^\lambda(\xi(x)) \right| \leq e^{-q_1\lambda}, \quad q_1 > 0.$$

(iii) **The Gibbs condition**
There exists a number $\beta < 1$ such that if λ is proportional to N we have

$$\left| < \phi_l^\lambda(\xi), \Psi_k(x(\xi)) >_\lambda \right| \max_{-1\leq\xi\leq 1} \left|\phi_l^\lambda(\xi)\right| \leq \left(\frac{\alpha N}{k}\right)^\lambda, \quad k > N, \quad l \leq \lambda, \quad \alpha < 1.$$

Orthonormality makes sure to avoid redundancy. Thus to describe a function with only a small amount of coefficients. The spectral convergence condition ensures that the maximum difference between the actual function and the approximation converges exponentially. In other words, the “new” approximation does not exhibit the Gibbs phenomenon. Finally, the Gibbs condition makes sure that the new projection basis can contain all the necessary information about the function that needs to be approximated. This means that we can project the high modes of the basis $\{\Psi_k\}$ (with $k > N$) on the low modes of the Gibbs complementary family ϕ_l^λ (with small l).

To conclude, a slowly converging series

$$\tilde{f}_N(x) = \sum_{k=0}^{N} (f, \Psi_k)\Psi_k(x), \tag{5.17}$$

can still yield a rapidly converging approximation to $f(x)$ if one can find another reprojection basis that satisfies the above three conditions. Hence, given the locations of the jump discontinuities, we can reconstruct partially analytic functions using spectral reprojection methods.

An example of a Gibbs complementary family are the Gegenbauer polynomials. In the next chapter it will be demonstrated that any Fourier approximation can be re-expanded in the Gegenbauer basis. This method is known as the Gegenbauer reconstruction method and the newly constructed approximation converges exponentially.

6

Gegenbauer Reconstruction Method

As we have seen before, piecewise analytic functions exhibit the Gibbs phenomenon, resulting in oscillations near the "jumps" and only first-order accuracy away from the jump discontinuities. One way to reduce the Gibbs phenomenon is to reproject the Fourier series on another set of basis functions. In this chapter we will discuss an example of such a reprojection method: the Gegenbauer reconstruction method.

First of all, we will show that the Gegenbauer reconstruction method can remove the Gibbs phenomenon for an analytic, non-periodic function $f \in L^2[-1,1]$ with a single jump discontinuity. After that, we will summarize this result in the main resolution theorem. Finally, we will look at the case of multiple jump discontinuities (as we have seen in Chapter 4) by considering an analytic function $f \in L^2[-1,1]$ that is analytic on a sub-interval $[a,b] \subset [-1,1]$.

Throughout this chapter we will use N to denote the number of Fourier coefficients. Furthermore, m denotes the polynomial order of the Gegenbauer reconstruction, thus $m+1$ will be the number of Gegenbauer coefficients used in the "new" approximation and λ is the parameter that determines the weight function of the Gegenbauer polynomials.

6.1. Resolution using Gegenbauer polynomials

The Gegenbauer transform can be seen as a special case of the Fourier transform, which is a projection on a set of orthogonal basis functions. The Gegenbauer projection uses Gegenbauer polynomials instead of the functions e^{int} (in Fourier expansion), as a basis.

6.1.1. Gegenbauer polynomials

The Gegenbauer polynomials $C_n^\lambda(x)$ are solutions to the differential equation

$$(1-x^2)y'' - 2(\lambda+1)xy' + n(n+2\lambda)y = 0. \tag{6.1}$$

They are defined as

Definition 6.1. The Gegenbauer polynomials $C_n^\lambda(x)$ for $\lambda \geq 0$ are the polynomial of order n that satisfy

$$\int_{-1}^{1} (1-x^2)^{\lambda-\frac{1}{2}} C_k^\lambda(x) C_n^\lambda(x) dx = 0 \quad \text{for} \quad k \neq n,$$

with normalization

$$C_n^\lambda(1) = \frac{\Gamma(n+2\lambda)}{n!\Gamma(2\lambda)}.$$

If we consider a function $f(x)$ on the interval $[-1,1]$, we define its Gegenbauer coefficients as

$$\hat{f}_l^\lambda(x) = \frac{1}{h_l^\lambda}\int_{-1}^{1}(1-x^2)^{\lambda-\frac{1}{2}}f(x)C_l^\lambda(x)dx, \tag{6.2}$$

with

$$h_l^\lambda = \pi^{\frac{1}{2}}C_n^\lambda(1)\frac{\Gamma\left(\lambda+\frac{1}{2}\right)}{n!\Gamma(\lambda)(l+\lambda)}. \tag{6.3}$$

Furthermore, we define the truncated Gegenbauer series expansion of $f(x)$ based on the first $m+1$ terms as

$$G_m^\lambda(f)(x) := \sum_{l=0}^{m}\hat{f}_l^\lambda(x)C_l^\lambda(x). \tag{6.4}$$

Hence, the Gegenbauer polynomials are polynomials of order m which are orthogonal with respect to their weight function $(1-x^2)^{\lambda-\frac{1}{2}}$ in the interval $[-1,1]$, i.e.

$$\int_{-1}^{1}(1-x^2)^{\lambda-\frac{1}{2}}f(x)C_k^\lambda(x)C_l^\lambda(x)dx = \delta_{k,l}h_l^\lambda. \tag{6.5}$$

The Gegenbauer series G_m^λ has two parameters; m describes the polynomial order of the Gegenbauer expansion and the parameter λ determines the weight function. These parameters play an important role in estimating the truncation and regularization error of the Gegenbauer approximation.

6.1.2. Procedure

Let $f(x) \in L^2[-1,1]$ be an arbitrary function. Assume that the first $2N+1$ Fourier coefficients $\hat{f}(n)$ are given, thus $S_N[f](x)$ as defined in (2.5) is known.
The idea is to construct an exponential convergent approximation by using a Gegenbauer expansion based on the information that is contained in the first $2N+1$ Fourier coefficients. This procedure consists of two steps.

Step 1:
We want to recover the first $m+1$ Gegenbauer coefficients, defined as in (6.2). Since the function $f(x)$ is unknown, we only have an approximation of the Gegenbauer coefficients $\hat{f}_l^\lambda$ of the original function. This approximation is denoted by $\hat{g}_l^\lambda$ and can be obtained by using the partial Fourier sum

$$\hat{g}_l^\lambda = \frac{1}{h_l^\lambda}\int_{-1}^{1}(1-x^2)^{\lambda-\frac{1}{2}}S_N[f](x)C_l^\lambda(x)dx. \tag{6.6}$$

Step 2:
We want to construct a Gegenbauer expansion from the obtained Gegenbauer coefficients $\hat{g}_l^\lambda$ in the previous step. Assume that $f(x)$ is an analytic function on $[-1,1]$ satisfying the following assumption.

Assumption 6.1. *There exist constants $\rho \geq 1$ and $C(\rho)$ such that, for every $k \geq 0$,*

$$\max_{-1\leq x\leq 1}\left|\frac{d^k f}{dx^k}(x)\right| \leq C(\rho)\frac{k!}{\rho^k},$$

where ρ is the distance from $[-1,1]$ to the nearest singularity of $f(x)$ in the complex plane.

Then we can denote $G_m^\lambda(f)(x)$ as the Gegenbauer expansion based on the first $m+1$ Gegenbauer coefficients $\hat{g}_l^\lambda$

$$G_m^\lambda(f)(x) = \sum_{k=0}^{m}\hat{g}_l^\lambda C_l^\lambda(x). \tag{6.7}$$

6.1.3. Exponential convergence

Now we must show that we have exponential accuracy in obtaining the Gegenbauer coefficients during the first step, provided that m and λ are proportional to N. Furthermore, we need to show that the constructed Gegenbauer expansion in step 2 also converges exponentially with N, given that the original function is analytic, but contains a single jump discontinuity.

Let F_m^λ be the expansion of the original function $f(x)$ into m-th degree Gegenbauer polynomials:

$$F_m^\lambda = \sum_{l=0}^{m} \hat{f}_l^\lambda C_l^\lambda(x), \tag{6.8}$$

where we defined $\hat{f}_l^\lambda$ as the Gegenbauer coefficients of the original function.

Truncation error

During the first step of the procedure we obtained the following truncation error T_e.

$$T_e := ||F_m^\lambda - G_m^\lambda|| = \max_{-1\leq x\leq 1} \left| \sum_{l=0}^{m} \left(\hat{f}_l^\lambda - \hat{g}_l^\lambda\right) C_l^\lambda(x) \right| \tag{6.9}$$

The truncation error is defined as the difference between the Gegenbauer expansion (with $m+1$ terms) of the function $f(x)$ and the truncated Fouries series $S_N[f](x)$. Thus it measures the error in the finite Gegenbauer expansion due to truncating the Fourier series.

The following theorem from [7] shows that if both λ and m grow linearly with N the truncation error can be made exponentially small.

Theorem 6.1 (Exponential decay of truncation error)**.** *Let $f(x)$ be a function in $L^2[-1,1]$, and its Fourier coefficients $\hat{f}(n), -N \leq n \leq N$ defined as in (5.1). Let $\hat{f}_l^\lambda$ be the Gegenbauer coefficients of $f(x)$ as defined in (6.2) and $\hat{g}_l^\lambda$ be the Gegenbauer coefficients of the partial Fourier sum $S_N[f](x)$ defined in (6.6).*
Then, if $\lambda = \alpha N$ and $m = \beta N$ for $\alpha, \beta > 0$, the truncation error decays exponentially with N, i.e.

$$T_e(\alpha N, \beta N, N) = \max_{-1\leq x\leq 1} \left| \sum_{l=0}^{m} \left(\hat{f}_l^\lambda - \hat{g}_l^\lambda\right) C_l^\lambda(x) \right| \leq AN^2 q_T^N,$$

with $q_T = \frac{(\beta+2\alpha)^{\beta+2\alpha}}{\beta^\beta (2e\pi\alpha)^\alpha}$.

Regularization error

The regularization error R_e originates from the second step of the procedure. Thus we consider a function $f(x)$ analytic on $[-1,1]$ and satisfying the assumption (6.1).

$$R_e := ||f - F_m^\lambda|| = \max_{-1\leq x\leq 1} \left| f(x) - \sum_{l=0}^{m} \hat{f}_l^\lambda C_l^\lambda(x) \right| \tag{6.10}$$

The regularization error can be estimated in the maximum norm by the following theorem from [7].

Theorem 6.2 (Exponential decay of regularization error)**.** *Let $f(x)$ be an analytic function on $[-1,1]$ satisfying assumption (6.1). Let $\hat{f}_l^\lambda, 0 \leq l \leq m$ be the Gegenbauer coefficients of $f(x)$ as defined in (6.2). Furthermore, if $\lambda = \alpha N$ and $m = \beta N$ for $\alpha, \beta > 0$. Then*

$$R_e(\alpha N, \beta N, N) = \max_{-1\leq x\leq 1} \left| f(x) - \sum_{l=0}^{m} \hat{f}_l^\lambda C_l^\lambda(x) \right| \leq Bq_R^N,$$

where $q_R = \frac{(\beta+2\alpha)^{\beta+2\alpha}}{\alpha^\alpha 2^{\beta+2\alpha} (\beta+\alpha)^{\beta+\alpha}}$.

To achieve exponential decay of the truncation error and regularization error, both the degree m and the weight parameter λ have to be selected proportional to N.

6.2. Main Resolution theorem

To summarize, with properly chosen parameters we can reconstruct an analytic (but non-periodic) function with exponential accuracy by using the Gegenbauer reconstruction method. Thus, we can construct an exponentially convergent approximation to an analytic, non-periodic function, from its first $2N+1$ Fourier coefficients.

This can be done by the procedure described in Subsection 6.1.2. In Subsection 6.1.3 we showed this approximation is exponentially accurate and thus converges to the true coefficients provided that λ grows linearly with N. Furthermore, these coefficients can be used to construct the partial Gegenbauer expansion which is shown to converge exponentially to $f(x)$. These results can be summarized in the following main resolution theorem about the removal of the Gibbs phenomenon.

Theorem 6.3 (Main resolution theorem)**.** *Consider an analytic and non-periodic function $f(x)$ on $[-1,1]$, satisfying*

$$\max_{-1\le x\le 1}\left|\frac{d^k f}{dx^k}(x)\right| \le C(\rho)\frac{k!}{\rho^k}, \quad \rho \ge 1.$$

Assume that the first $2N+1$ Fourier coefficients $\hat{f}(n)$ are known.
Let $\hat{g}_l^\lambda, 0 \le l \le m$, be the Gegenbauer coefficients of $S_N[f](x) = \sum_{n=-N}^{N} \hat{f}(n)e^{inx}$.
Then, for $\lambda = \alpha N$ and $m = \beta N$ with $\alpha, \beta > 0$

$$\max_{-1\le x\le 1}\left|f(x) - \sum_{l=0}^{m} \hat{g}_l^\lambda C_l^\lambda(x)\right| \le AN^2 q_T^N + Bq_R^N,$$

where

$$q_T = \frac{(\beta+2\alpha)^{\beta+2\alpha}}{\beta^\beta(2e\pi\alpha)^\alpha} < 1, \quad q_R = \frac{(\beta+2\alpha)^{\beta+2\alpha}}{\alpha^\alpha 2^{\beta+2\alpha}(\beta+\alpha)^{\beta+\alpha}} < 1.$$

Proof. The proof of exponential convergence involves considering the distance between the original function $f(x)$ and its approximation based on the Gegenbauer series $G_m^\lambda(f)(x)$.
More formally,

$$||f - G_m^\lambda|| \le ||f - F_m^\lambda|| + ||F_m^\lambda - G_m^\lambda||.$$

This equation can be rewritten in terms of the truncation error and regularization error as defined in (6.9) and (6.10) to obtain

$$\begin{aligned}\max_{-1\le x\le 1}\left|f(x) - \sum_{l=0}^{m} \hat{g}_l^\lambda C_l^\lambda(x)\right| &\le \max_{-1\le x\le 1}\left|f(x) - \sum_{l=0}^{m} \hat{f}_l^\lambda C_l^\lambda(x)\right| + \max_{-1\le x\le 1}\left|\sum_{l=0}^{m}\left(\hat{f}_l^\lambda - \hat{g}_l^\lambda\right) C_l^\lambda(x)\right| \\ &\le Bq_R^N + AN^2 q_T^N.\end{aligned}$$

The first term is the regularization error and the second term describes the truncation error. Both errors are bounded, as can be seen in Theorem 6.2 and Theorem 6.1 respectively. □

So far we can remove Gibbs oscillations from non-periodic analytic functions, thus handling a single jump discontinuity. However, what if the function has multiple jump discontinuities?

6.2.1. Reconstruction for piecewise analytic functions

For piecewise analytic functions one can project each analytic sub-interval on another basis and then combine these parts to restore the function on the whole interval. Let $f(x)$ be such a function in $L^2[-1,1]$, which is analytic on a sub-interval $[a,b] \subset [-1,1]$.
Just as in Section 5.3, we can use the linear transformation of $x \in [a,b]$ to $\xi \in [-1,1]$ and apply the Gegenbauer projection $G_m^\lambda(S_N[f])(\xi(x))$ in order to get the following expression for the Gegenbauer coefficients

$$\tilde{g}_l^\lambda = \frac{1}{h_l^\lambda}\int_{-1}^{1}(1-\xi^2)^{\lambda-\frac{1}{2}} S_N[f](\xi(x))C_l^\lambda(\xi)d\xi. \tag{6.11}$$

Hence, following the same procedure, we can obtain the Gegenbauer coefficients $\tilde{g}_l^\lambda$ by evaluating these integrals. Computing these integrals is more costly, but the idea remains the same: computing the Gegenbauer coefficients by using the given truncated Fourier series.

6.2.2. Gegenbauer reconstruction of step function

Consider the step function defined on $[-1, 1]$ of the form $f(x) = \frac{1}{2L}$ for $x \in [-L, L]$. To illustrate the Gegenbauer reconstruction compared to the Fourier reconstruction we will look at the approximation of this function using both methods. Furthermore, we will consider different values of the parameter m to show the importance of choosing the right amount of coefficients used in the Gegenbauer expansion.

In Figure 6.1, it can be seen that if the number of Fourier coefficients N (proportional to m) is too low, the reconstruction will not be accurate. However, if we take m too high, the reconstruction will still exhibit some of the Gibbs phenomenon as can be seen in Figure 6.2.

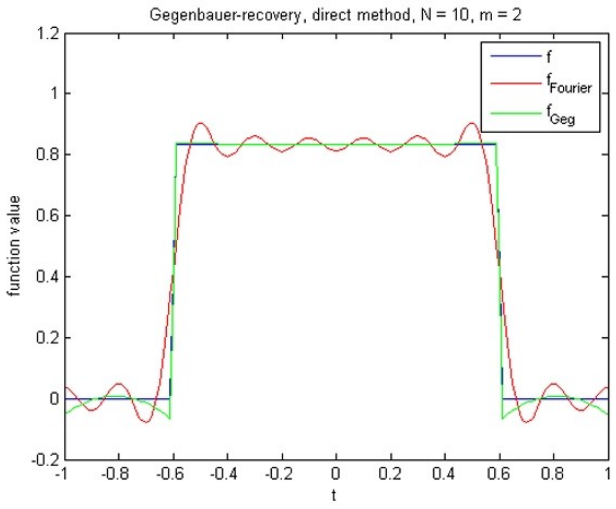

Figure 6.1: Gegenbauer reconstruction with not enough Fourier coefficients. Figure from [11].

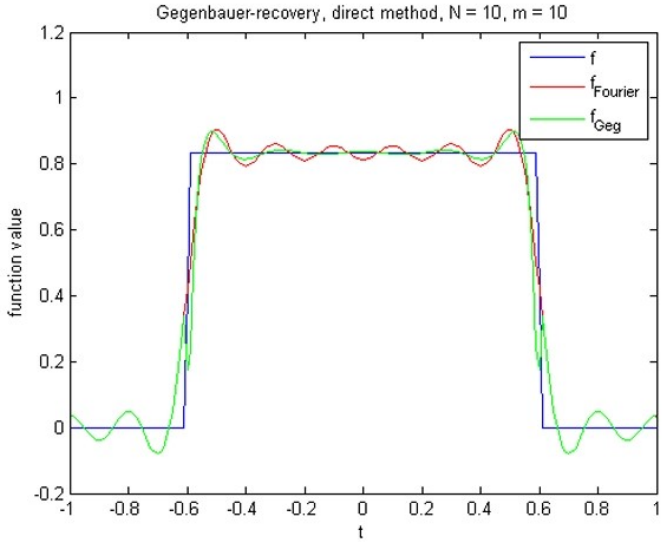

Figure 6.2: Gegenbauer reconstruction with m too high. Figure from [11].

To conclude, m has to have a value for which both the truncation error and regularization error decay exponentially. Figure 6.3 shows that if m is chosen carefully, then the Gegenbauer reconstruction indeed will be a good approximation of the original function.

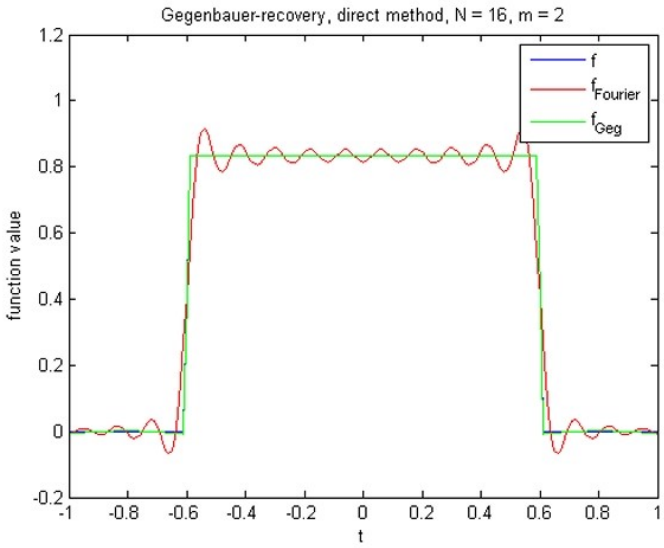

Figure 6.3: Gegenbauer reconstruction with parameters well chosen. Figure from [11].

7

Application to MRI

One of the most common applications of Fourier analysis is signal processing. The Fourier transform is often used to decompose a signal into individual simple sine and cosine waves with varying combinations of frequencies and amplitudes. By adding together all these simpler waves with their corresponding Fourier coefficients, the Fourier series, we can reconstruct the original signal. This enables us to approximate an infinite signal in the time domain with a finite amount of Fourier coefficients in the frequency domain.

7.1. Magnetic Resonance Imaging

Magnetic Resonance Imaging (MRI) is a noninvasive procedure that provides discrete data about the human body. With regard to MRI, the signal we wish to decompose is the MR echo containing the frequency-and phase-encoded spatial information necessary to construct an image.

This signal is digitized, decomposed by the Fourier transform, and entered into a two-dimensional Fourier space, the so-called 'k-space', that organizes spatial frequency and amplitude information [4]. One pixel in k-space corresponds to a single, specific spatial frequency. The two-dimensional inverse Fourier transform of the k-space combines all these spatial frequencies to obtain an image.

The filtered Fourier reconstruction method is mostly used to reconstruct the image. This Fourier approximation is commonly used because of its exponentially and uniformly converging approximation for images without discontinuities (or edges). However, if the image contains discontinuities, then spurious oscillations will appear in the reconstruction at the discontinuities and the overall convergence rate will be significantly reduced. This behaviour can be seen in the image and is called the Gibbs ringing artifact.

7.1.1. Gibbs ringing artifact

Gibbs artifact is an imperfect approximation of sharp edges by a Fourier series lacking an adequate number of high-frequency terms. In MRI, this is commonly referred to as the "ringing artifact". This artifact appears due to the many different tissues of the body present in each scan. It can be seen as an oscillation appearing radially around the borders of the image discontinuities. In axial brain imaging, the Gibbs ringing artifact manifests itself at the boundaries of the tissues as can be seen in Figure 7.1, making it difficult to determine the structure of the brain tissue.

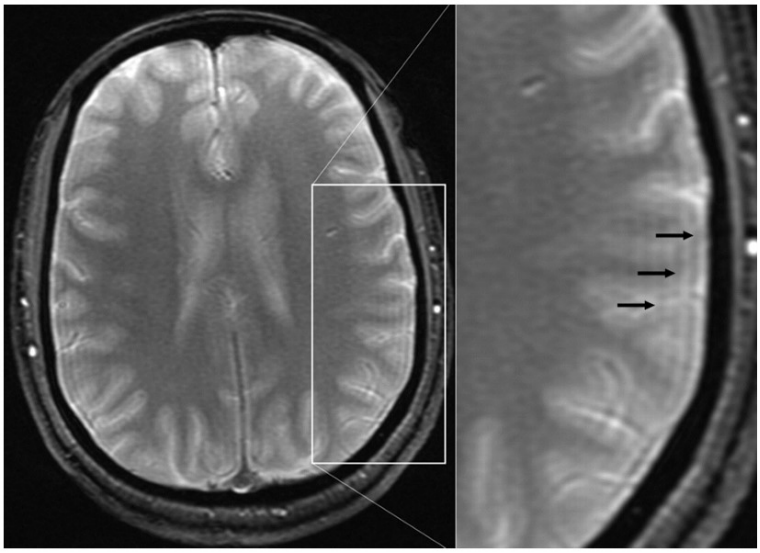

Figure 7.1: Gibbs artifact. Axial gradient-echo image of brain obtained at 256 x 160 matrix. Gibbs artifact near inner table of calvarium manifests as subtle hypointense lines overlying cortex (arrows), image from [4].

7.2. Resolution to Gibbs ringing artifact

In Neural imaging, there is a difference between high-signal fat in the scalp and low-signal in the scull. Therefore the underlying function has discontinuities at tissue boundaries and consequently the Gibbs ringing artifact will occur. Hence, we get oscillations near tissue boundaries and the overall rate of convergence will be reduced to first-order. To demonstrate a resolution of the Gibbs ringing artifact, we will be looking at the two-dimensional Fourier approximation of a piecewise analytic periodic function on $[-1,1]\times[-1,1]$ that is sampled on equally spaced discrete data points $x_j = \frac{j-N}{N}$ for $j = 0, ..., 2N-1$.

The two-dimensional Fourier approximation is given by

$$S_N[f](x,y) = \sum_{k=-N}^{N}\sum_{l=-N}^{N} \hat{f}_{k,l} e^{i(kx+ly)}, \tag{7.1}$$

where we define the Fourier coefficients as

$$\hat{f}_{k,l} = \frac{1}{4N^2 c_k c_l} \sum_{j=-0}^{2N-1}\sum_{h=-0}^{2N-1} f(x_j, y_h) e^{-i(kx_j+ly_h)}. \tag{7.2}$$

7.2.1. Filtered Fourier reconstruction

As noted in Section 5.2 a filter can increase the rate of decay of the Fourier coefficients away from the discontinuity. The filtered Fourier reconstruction applied to MRI is efficient and has low computational cost [1].

The two-dimensional filtered Fourier reconstruction is computed as

$$S_N^{\sigma}[f](x,y) = \sum_{k=-N}^{N}\sum_{l=-N}^{N} \sigma_k \sigma_l \hat{f}_{k,l} e^{i(kx+ly)}, \tag{7.3}$$

where $\sigma_k = \sigma\left(\frac{|k|}{N}\right)$ and $\sigma_l = \sigma\left(\frac{|l|}{N}\right)$ are the filter functions used.

However, this filtered Fourier reconstruction still exhibits oscillating behavior near the tissue boundaries. Thus, we will consider applying a hybrid method in which we combine the efficiency of filtered Fourier in regions away from discontinuities and the high-resolution of Gegenbauer reconstruction near the discontinuities.

7.2.2. Hybrid Gegenbauer method

In Chapter 6 we have seen that the Gegenbauer reconstruction method clearly has a higher resolution near jump discontinuities compared to the (filtered) Fourier approximation. However, it is considerably more computationally costly than the filtered Fourier reconstruction [1].

In order to perform the hybrid Gegenbauer method we must be able to locate the discontinuities and their corresponding jump values.Therefore an edge-detection method is necessary to determine the analytic intervals in which the images can be reconstructed, see for example [1].

Let both x and y be close to the edges of the interval, so near the discontinuities, then we apply the Gegenbauer reconstruction procedure in both directions.

The Gegenbauer coefficients in two dimensions can be computed as

$$\hat{g}_{k,l}^{\lambda} = \frac{1}{h_k^{\lambda} h_l^{\lambda}} \int_{-1}^{1} \int_{-1}^{1} (1-\eta_x^2)^{\lambda-\frac{1}{2}} (1-\eta_y^2)^{\lambda-\frac{1}{2}} S_N[f]\left(x(\eta_x), y(\eta_y)\right) C_k^{\lambda}(\eta_x) C_l^{\lambda}(\eta_y) d\eta_x \eta_y, \tag{7.4}$$

where η_x and η_y are the local variables in $[-1,1]$ defined by $x(\eta_x) = \varepsilon_x \eta_x + \delta_x$ and $y(\eta_y) = \varepsilon_y \eta_y + \delta_y$ with $\varepsilon_x = \frac{(b_x - a_x)}{2}$, $\varepsilon_y = \frac{(b_y - a_y)}{2}$ and $\delta_x = \frac{(b_x + a_x)}{2}$, $\delta_y = \frac{(b_y + a_y)}{2}$.
The Gegenbauer coefficients are computed using the two-dimensional Fourier partial sum $S_N^{\sigma}[f](x(\eta_x), y(\eta_y))$ as can be computed in (7.1).

Furthermore, we can construct the two-dimensional Gegenbauer series. For simplicity, assume we choose $\lambda = \lambda_x = \lambda_y$ and $m = m_x = m_y$. Then using the Gegenbauer reconstruction methods in both directions we get

$$G_m^{\lambda,\theta}(f)(x,y) = \sum_{k=0}^{m} \sum_{l=0}^{m} \hat{g}_{k,l}^{\lambda}(x) C_k^{\lambda}(x) C_l^{\lambda}(y). \tag{7.5}$$

Consider a piecewise analytic function $f(x)$ that is analytic inside the interval $[a_x, b_x] \times [a_y, b_y]$. Then the hybrid Gegenbauer method is given by

$$h_m^{\sigma,\lambda,\theta}(x,y) = \begin{cases} G_m^{\lambda,\theta}(f)(x,y) & \text{if} \quad a_x \le x \le a_x + \rho, \quad a_y \le y \le a_y + \rho \\ & \text{or} \quad b_x - \rho \le x \le b_x, \quad b_y - \rho \le y \le b_y \\ S_N^{\sigma}[f](x,y) & \text{if} \quad a_x + \rho < x < b_x - \rho \quad \text{and} \quad a_y + \rho < y < b_y - \rho \end{cases}, \tag{7.6}$$

where $0 \le \rho \le \frac{(b-a)}{2}$ is a neighborhood parameter.

Thus, inside the analytic interval we will use the computational efficient two-dimensional filtered Fourier partial sum and in the neighborhood of a jump discontinuity we use the high-resolution Gegenbauer method. To conclude, it is possible to improve the accuracy of reconstruction in MRI by using the hybrid Gegenbauer method.

8

Conclusion

In this report, we showed the existence of the Gibbs phenomenon for the Saw-tooth wave function and computed the size of the overshoot and undershoot near the jump discontinuities by evaluating the sine integral function. In particular, we observed that this overshoot and undershoot will never decrease below 9% of the height of the "jump".

Using the convergence result from the uniform Riemann Lesbesgue Lemma, we showed that any piecewise smooth function with a jump discontinuity at the origin exhibits this phenomenon. After that, we generalized this result for a function with a jump discontinuity at a general point.
Hence, we showed that any piecewise smooth function with a finite number of jump discontinuities exhibits the Gibbs phenomenon.

The Gibbs phenomenon arises when we approximate a function with a jump discontinuity. Specifically, the convergence of the Fourier coefficients to zero deteriorates to the first order and spurious oscillations develop near the jump discontinuities. In the second part of this thesis we discussed several techniques to remove these oscillations and improve the convergence rate.
Filtering methods can improve the convergence rate away from the jump discontinuities, however this will not improve the non-uniform convergence near the "jumps". In order to completely remove the Gibbs phenomenon we need to re-expand the Fourier approximation using a different set of basis functions. Spectral reprojection methods can be used to reconstruct a rapidly converging series from the knowledge of the Fourier coefficients by using a "Gibbs complementary family" of expansion functions. These reprojection methods are very suitable for recovering piecewise analytic functions from their Fourier coefficients with great accuracy up to the jump discontinuities.
For example, we have seen that the Gegenbauer reconstruction method can be used to reconstruct an exponentially convergent approximation of a piecewise analytic function.

Finally, we looked at the occurrence of Gibbs ringing artifact in Magnetic Resonance Imaging. It has been shown that it is possible to improve the accuracy of image reconstruction by using the hybrid Gegenbauer method. This method combines the efficiency of the filtered Fourier reconstruction in regions away from the tissue boundaries and the high-resolution of the Gegenbauer reconstruction near the tissue boundaries.

Discussion and further research

It is possible to study other possible Gibbs complementary basis functions that can further improve the accuracy. In particular, one can try to address the weaknesses of the Gegenbauer reconstruction method that consist of round-off errors and the appearance of the generalized Runge phenomenon.
In addition, one can demonstrate the improvement of the Gibbs ringing artifact in medical imaging for the MRI by simulating brain phantoms.
Furthermore, different edge-detection methods, necessary in order to apply the hybrid Gegenbauer method in MRI, could be reviewed.

References

[1] R. Archibald and A. Gelb. “A method to Reduce the Gibbs Ringing Artifact in MRI scans While Keeping Tissue Boundary Integrity”. In: *IEEE Transactions on Medical imaging* 21.4 (2002).

[2] A.C. Hansen B. Adcock. “A Generalized Sampling Theorem for Stable Reconstructions in Arbitrary Bases”. In: *Journal of Fourier Analysis and Applications* 18 (2012).

[3] M. Bôcher. “Introduction to the theory of Fourier’s series”. In: *Ann. of Math. Monthly* 7 (1905-1906), pp. 81–152.

[4] T.A. Gallagher, A.J. Nemeth, and L. Hacein-Bey. “An Introduction to the Fourier Transform: Relationship to MRI”. In: *American Journal of Roentgenology* 190.5 (2008), pp. 1396–1405.

[5] J. W. Gibbs. “Letter”. In: *Nature* 59 (1898-1899), pp. 123–456.

[6] D. Gottlieb and C. Shu. “On the Gibbs phenomenon and its resolution”. In: *Society for Industrial and Applied Mathematics Rev.* 39.4 (1997), pp. 644–668.

[7] D. Gottlieb, C. Shu, and A. Solomonoff. “On the Gibbs phenomenon I: recovering exponential accuracy from the Fourier partial sum of a nonperiodic analytic function”. In: *Journal of computational and applied mathematics* (1992).

[8] S. Gottlieb and A. Gelb. “The resolution of the Gibbs phenomenon for Fourier spectral methods”. In: *Advances in the Gibbs phenomenon, Sampling publishing, Potsdam* (2007).

[9] T.W. Körner. *Fourier analysis*. Cambridge: Cambridge University Press, 1988.

[10] E. Stein and R. Shakarchi. *Fourier analysis; an introduction*. Princeton, NJ: Princeton University Press, 2003.

[11] M. Versteegh. “The Gibbs phenomenon in option pricing methods”. In: *A thesis submitted to DIAM* (2012).

[12] A. Vretblad. *Fourier analysis and its applications*. Uppsala university: Graduate Texts in Mathematics, 2000.

[13] H. Wilbraham. “On a certain periodic function”. In: *Cambridge Dublin Math. Journal* 3 (1848), pp. 198–201.

A

Appendix

A.1. Riemann-Lebesgue Lemma

Lemma A.1. *Let $-\infty \leq a < b \leq \infty$ and $f \in L^1(a,b)$. Then*

$$\lim_{|\lambda| \to \infty} \int_a^b f(x) e^{-i\lambda t} dt = 0. \tag{A.1}$$

In particular, if $f \in L^1(\mathbb{T})$, then $\hat{f}(n) \to 0$ as $|n| \to \infty$.

Proof. For all $\lambda \in \mathbb{R}$ we consider

$$\mathbb{J}(f, \lambda) = \frac{1}{2\pi} \int_{-\pi}^{\pi} f(t) e^{-i\lambda t} dt.$$

Observe that $\mathbb{J}(f,\lambda)$ is well-defined since we have

$$|\mathbb{J}(f,\lambda)| \leq \frac{1}{2\pi} \int_{-\pi}^{\pi} |f(t)||e^{-i\lambda t}| dt = ||f||_1 < \infty.$$

The structure of the proof consists of three parts. First, the statement (A.1) will be proven for characteristic functions. Secondly, simple functions will be considered and finally the density of simple functions in $L^1(-\pi,\pi)$ will be used in order to proof (A.1) for functions $f \in L^1(-\pi,\pi)$.

Let $\alpha, \beta \in \mathbb{R}$ with $-\pi < \alpha < \beta \leq \pi$, and denote

$$\mathbf{1}_{[\alpha,\beta)}(t) = \begin{cases} 1 & \text{if } t \in [\alpha,\beta) \\ 0 & \text{else} \end{cases} .$$

Then for $\lambda \neq 0$, we have

$$\mathbb{J}(\mathbf{1}_{[\alpha,\beta)}, \lambda) = \frac{1}{2\pi} \int_{-\pi}^{\pi} \mathbf{1}_{[\alpha,\beta)}(t) e^{-i\lambda t} dt = \frac{1}{2\pi} \int_{\alpha}^{\beta} e^{-i\lambda t} dt = -\frac{1}{2\pi i \lambda} \left(e^{-i\lambda\beta} - e^{-i\lambda\alpha} \right). \tag{A.2}$$

Thus if we take the limit $|\lambda| \to \infty$ we get

$$\begin{aligned} \lim_{|\lambda| \to \infty} |\mathbb{J}(\mathbf{1}_{[\alpha,\beta)}, \lambda)| &= \lim_{|\lambda| \to \infty} \frac{|e^{-i\lambda\beta} - e^{-i\lambda\alpha}|}{2\pi|\lambda|} \\ &\leq \lim_{|\lambda| \to \infty} \frac{2}{2\pi|\lambda|} \\ &= \lim_{|\lambda| \to \infty} \frac{1}{\pi|\lambda|} = 0. \end{aligned} \tag{A.3}$$

Hence, we proved the statement (A.1) for characteristic functions.

Consider step functions defined as

$$s = \sum_{i=1}^{n} \gamma_i \mathbf{1}_{[\alpha_i, \beta_i)},$$

for $-\pi < \alpha_i < \beta_i \leq \pi$. By linearity of the integral, it follows from (A.3) that

$$\lim_{|\lambda| \to \infty} \mathbb{J}(s, \lambda) = \sum_{i=1}^{n} \gamma_i \mathbb{J}\left(\mathbf{1}_{[\alpha_i, \beta_i)}, \lambda\right) = 0. \tag{A.4}$$

Finally, let $f \in L^1(-\pi, \pi)$.
Since step functions are dense in $L^1(-\pi, \pi)$ we get for all $\epsilon > 0$ there exists $s_\epsilon = \sum_{i=1}^{n} \gamma_i \mathbf{1}_{[\alpha_i, \beta_i)}$ such that $||f - s_\epsilon||_1 < \frac{\epsilon}{2}$. Furthermore, from the second part of the proof (A.4) we know there exists $\delta_\epsilon > 0$ such that for all $|\lambda| > \delta_\epsilon$ we have $|\mathbb{J}(s, \lambda)| < \frac{\epsilon}{2}$.
Combining these two results we get that for all $|\lambda| > \delta_\epsilon$, we have

$$\begin{aligned} |\mathbb{J}(f, \lambda)| &\leq |\mathbb{J}(f - s, \lambda)| + |\mathbb{J}(s, \lambda)| \\ &\leq ||f - s||_1 + |\mathbb{J}(s, \lambda)| \\ &< \frac{\epsilon}{2} + \frac{\epsilon}{2} = \epsilon. \end{aligned} \tag{A.5}$$

To conclude, we proved that

$$\lim_{|\lambda| \to \infty} \mathbb{J}(f, \lambda) = 0.$$

□

A.2. Additional theorem for proving the Gibbs phenomenon

Theorem A.1. *For $0 \leq l \leq \left[\frac{1}{2}(n-1)\right] - 1$, we have*

$$\phi_n\left(\frac{2l+1}{n+1}\pi\right) > \phi_n\left(\frac{2l+3}{n+1}\pi\right).$$

Proof. Define

$$\psi_\pm(t) = \phi_n\left(\frac{(2l+2)\pi \pm t}{n+1}\right) \tag{A.6}$$

and

$$\omega(t) = \psi_-(t) - \psi_-(t - 2\pi) - \psi_+(t) + \psi_+(t + 2\pi). \tag{A.7}$$

To show $\omega(t)$ is strictly increasing for $0 \leq t \leq \pi$, we consider

$$\frac{d\omega}{dt}(t) = \frac{\sin\left(\frac{1}{n+1}\pi\right)\sin(t)}{n+1}\left[\frac{1}{\cos\left(\frac{1}{n+1}\pi\right) - \cos\left(\frac{(2l+3)\pi - t}{n+1}\right)} - \frac{1}{\cos\left(\frac{1}{n+1}\pi\right) - \cos\left(\frac{(2l+3)\pi + t}{n+1}\right)}\right] \tag{A.8}$$

The full derivation of this equation can be found below in (**??**).
If n is even, the condition $0 \leq l \leq \left[\frac{1}{2}(n-1)\right] - 1$ implies $2l + 3 \leq n - 1$.
If n is odd, the condition implies $2l + 3 \leq n$.
Hence, we get

$$\cos\left(\frac{1}{n+1}\pi\right) > \cos\left(\frac{(2l+3)\pi - t}{n+1}\right) > \cos\left(\frac{(2l+3)\pi + t}{n+1}\right). \tag{A.9}$$

From inequality (A.9) we can conclude that in both cases (n is odd or even) the denominator of (A.8) is positive. So $\frac{d\omega}{dt}(t) > 0$ for $0 \leq t \leq \pi$. Consequently, $\omega(t)$ is strictly increasing on the interval $[0, \pi]$.

Since $\omega(0) = 0$, we get $\omega(\pi) > 0$.
From this inequality, we can obtain the following equation by using the definition of $\omega(t)$ from (A.7)

$$\phi_n\left(\frac{2l+3}{n+1}\pi\right) - \phi_n\left(\frac{2l+5}{n+1}\pi\right) < \phi_n\left(\frac{2l+1}{n+1}\pi\right) - \phi_n\left(\frac{2l+3}{n+1}\pi\right). \tag{A.10}$$

Now it is useful to consider two cases:

Case 1: n is even
If we consider $2l+3 = n-1$, we get $\phi_n\left(\frac{2l+5}{n+1}\pi\right) = \phi_n(\pi) = 0$. Substituting this in equation (A.10), we get

$$0 < \phi_n\left(\frac{n-1}{n+1}\pi\right) < \phi_n\left(\frac{n-3}{n+1}\pi\right) - \phi_n\left(\frac{n-1}{n+1}\pi\right). \tag{A.11}$$

Case 2: n is odd
If we consider $2l+3 = n$, we get $\phi_n\left(\frac{2l+5}{n+1}\pi\right) = \phi_n\left(\frac{n+2}{n+1}\pi\right)$. Substituting this in equation (A.10) we obtain

$$0 < \phi_n\left(\frac{n}{n+1}\pi\right) < \phi_n\left(\frac{n-1}{n+1}\pi\right) - \phi_n\left(\frac{n+2}{n+1}\pi\right) < \phi_n\left(\frac{n-2}{n+1}\pi\right) - \phi_n\left(\frac{n}{n+1}\pi\right). \tag{A.12}$$

Combining (A.10) with (A.11) for n is even and with (A.12) for n is odd finalizes the proof. □

A.3. Python code

Python code for Figures 3.3 and 3.4, to provide a visualization of the Gibbs phenomenon for the Saw-tooth wave function.

```python
import numpy as np
import matplotlib.pyplot as plt

# Define the nth partial sum function of Saw-tooth wave function
def nth_partial_sum(x, n):
    partial_sum = np.zeros_like(x)
    for k in range(1, n + 1):
        partial_sum += np.sin(k * x) / k
    return partial_sum

# Generate x values
x_values = np.linspace(0, np.pi, 1000)

# Number of terms in Fourier series
N = 250

# Calculate Nth-partial sum
S_N = nth_partial_sum(x_values, N)

# Plotting
plt.figure(figsize=(10, 6))
plt.plot(x_values, S_N)
plt.legend()
plt.grid(False)
plt.show()
```